PEM FUEL CELL AND ENERGY STORAGE UNIT CONFIGURATION FOR VEHICLE APPLICATIONS

By

Kalpana Thota

Problem Report Submitted to the College of Engineering and Mineral Resources
at West Virginia University

In partial fulfillment of the requirements for the degree of
MASTER OF SCIENCE
In
ELECTRICAL ENGINEERING

Approved by
Dr. Muhammad A Choudhry, Committee Chair
Dr. Roy Nutter
Dr. Brian Woerner

Lane Department of Computer Science and Electrical Engineering
Morgantown, West Virginia
2007

Keywords: PEM fuel cell, Energy storage unit, Battery, ultracapacitor, DC-DC converter, parallel configuration

Abstract

PEM FUEL CELL AND ENERGY STORAGE UNIT CONFIGURATION FOR VEHICLE APPLICATIONS

Kalpana Thota

In the current "future" automobile market; fuel cells have shown to be an alternative to the classic power sources like internal combustion engines. But in particular Polymer electrolyte membrane (PEM) fuel cells are used in the transportation applications. Automobiles have fast changing load requirements, while fuel cells have a slow dynamic response and cannot respond to the instantaneous loads. Additional energy is required to meet the changing load and hence improve the performance of the hybrid vehicle. An energy storage unit with a battery and/or an ultracapacitor can provide the additional energy to meet the increased load.

The load requirements for a mid size SUV are considered for the analysis. A simulink model of a PEM fuel cell is investigated and results are obtained from the simulations. An energy storage unit with a battery, ultracapacitor and DC-DC converters is designed to meet the instantaneous load requirements of the vehicle. The energy storage unit is simulated for the results. A parallel configuration of PEM fuel cell and a battery is also studied and modeled to observe the load sharing between the two units.

This thesis is dedicated to my family, Prem Reddy, Ramesh Babu Thota, Nirmala Thota, Karthik Thota, Nageshwar Rao Kolla, Ramakrishna Reddy and Vijitha whose love and support made this possible.

Acknowledgements

I would like to take this opportunity to express my cordial gratefulness to my advisor Dr. Muhammad A Choudhry who devoted immense time and effort in this Problem Report. I very much appreciate his great patience and tolerance. It has been my pleasure to work with a farsighted advisor like Dr. Choudhry.

I would also like to thank my Committee members Dr. Roy Nutter and Dr. Brian Woerner for their help.

I would like to thank my fiancé, Prem Reddy who provided insights, ideas and criticisms that made this Report possible. He has been a great source of motivation and inspiration.

I would like to thank my father who has always been for making sacrifices along the way to help me achieve my goals. I would like to thank my mother; my brother and my grand parents for providing unlimited love and enthusiasm. I would also like to thank my In-Laws and Preethi for their support and understanding.

Table of Contents

List of Figures

List of Tables

Chapter 1

INTRODUCTION

1.1 General Introduction

In recent years, automobiles powered by pure internal combustion engines are evolving into hybrid electric cars and thus leading to the advancement of better and faster engines. But during those years various environmental problems have come to our attention. About 25% to 75% of the chemicals that pollute air are emitted from transportation vehicle. Air pollution has been a serious threat for many years. Apart from air pollution the limited supply of natural resources has also come to attention i.e. particularly oil supply. Due to these factors non polluting energy sources have been acquiring a great deal of attention during the last few years. Several hybrid vehicles such as methanol-run cars and battery operated cars have been tested but they face several performance and production challenges. In the current "future" automobile market fuel cells have been showing as an alternative to the classic power sources due to their low impact on the environment, safe chemical properties, efficiency, reliability, applications and performances. Hence hydrogen fuel cell proves to be the best choice of alternative fuel compared to internal combustion engine.

Proton exchange membrane fuel cells are used primarily for transportation applications due to their fast start up time and favorable power to weight ratio.

1.2 Objective

Automobiles have fast changing load requirements while fuel cells have slow dynamic response and do not have enough capacity to respond to the fast changing loads.

This report is an attempt to simulate an auxiliary storage unit which can respond to the increased load instantaneously. An ultra capacitor and battery combination can be effective auxiliary storage unit because of its advantages such as high power density, long life cycle and very good charge and discharge efficiency. Also, this combination can provide large transient power instantly and hence provides power for increased load for automobile requirements like acceleration or sudden slope changes.

1.3 Background and Literature review of the PEM Fuel Cell:

1.3.1 Introduction

A fuel cell is an electrochemical energy conversion device. A fuel cell converts the chemicals hydrogen and oxygen into water, and in the process it produces electricity. The other electrochemical device that we are all familiar with is the battery. A battery has all of its chemicals stored inside, and it converts those chemicals into electricity too. This means that a battery eventually "goes dead" and you either throw it away or recharge it.

With a fuel cell, chemicals constantly flow into the cell so it never goes dead, as long as there is a flow of chemicals into the cell, the electricity flows out of the cell. Most fuel cells in use today use hydrogen and oxygen as the chemicals.

1.3.1.1 Basic Principles of Operation

The fuel cell is an electrochemical system which converts the chemical energy of a conventional fuel, directly into D.C. electrical energy [1]. The basic principle of operation is illustrated in Figure 1.1. A fuel cell comprises two porous electrodes, with a conducting electrolyte between them. At the anode, the hydrogen gives up electrons to the electrode, and enters the electrolyte as a positive ion (H^+), while at the cathode, the oxygen takes electrons and enters the electrolyte as a negative ion (O^{2-} or OH^-). The respective ions combine in the electrolyte and form water, while the electrons move through the external circuit, to produce electric current. Since these systems do not rely on thermal energy conversion, they are not bounded by Carnot efficiency limitations.

When fuel other than hydrogen is used, fuel processing or reforming is required. The role of the reformer is to convert any fuel into a hydrogen rich stream of gas. This is attained by mixing the fuel with steam (typical steam-to-carbon-ratio: 2.5). An additional role of fuel processing, is to ensure that CO is converted to CO_2 *(gas shift conversion)*. Thus, steam temperature has to be high enough to favor the above chemical reaction.

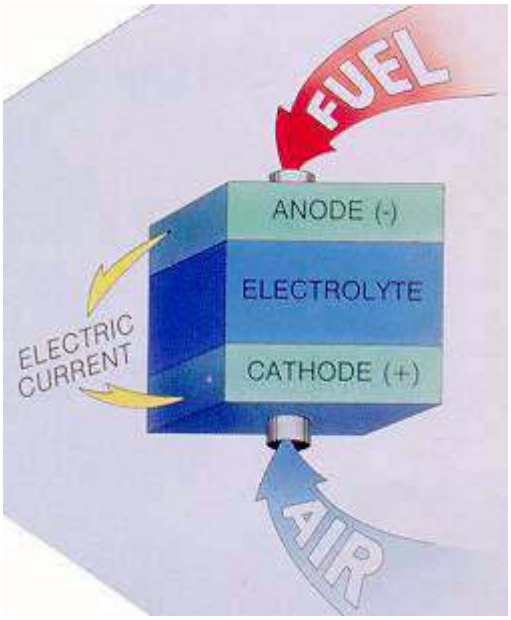

Fig 1.1 Fuel Cell–Principle of Operation [1].

Fuel cell system has fuel cell stacks where fuel cell modules are stacked to increase the power capacity of the system

1.3.2 Advantages of Fuel Cells

High Efficiency

As mentioned above, Fuel Cells are not bounded by the thermodynamic laws that limit Carnot cycle efficiencies. This is due to the fact that chemical energy of a fuel is directly converted into electricity, without intermediate conversion into heat, as in conventional power schemes. Hence, theoretical FC efficiencies reach 83 %. However, practical values (without heat recovery) are about 50 % [1].

High Responsivity

A fuel cell is capable of being switched-on and operates at full power, in 30 milli seconds.

High Reliability and Low Maintenance

Because of their simplicity of operation and the absence of moving parts, fuel cells are very reliable and need only 1/4 of the routine maintenance of conventional systems. Additional components, such as blowers are highly reliable, because of their wide use in industry.

Long Life

Fuel cells have a projected life of 40,000 h of operation at full load.

Fuel Flexibility

The ideal fuel for optimum Fuel Cell operation is hydrogen, although any material that can undergo an oxidation reaction can be used as fuel for a FC system. The following fuels are possibilities:

- Methane
- Propane
- Methanol
- Ethanol
- Natural Gas
- Biogas
- Petroleum
- Coal
- Naptha

Flexibility in Size and Applications.

The current produced from a fuel cell is proportional to the electrode area, and the potential output can be increased to meet the necessary power levels, by stacking Fuel Cell (FC) in piles.

Depending on its size and electrical output, a FC system can be used for a variety of applications ranging from micro-scale power generation for modular buildings to large-scale power generation.

No Noise and Pollution Free

The only source of noise is the small blowers that are used for cooling and supplying the cell with air. The SOx and NOx emissions are negligible, while emission of greenhouse gases is much lower compared to conventional power generation schemes.

1.3.3 Disadvantages:

The disadvantages are high costs compared to other energy systems technology and operation requires replenishable fuel supply.

1.4 Polymer Electrolyte Fuel Cell (PEM Fuel Cell)

The classification of the fuel cells is generally done on the basis of electrolyte being used. They also differ by their operating temperatures, materials and type of chemical reaction taking place. These characteristics help in determining the applications of a particular fuel cell.

Polymer electrolyte fuel cell uses a solid polymer as an electrolyte. The membrane is made up of Nafion, an excellent conductor of protons and an insulator of electrons. These have high power density and hence preferred for automotive applications.

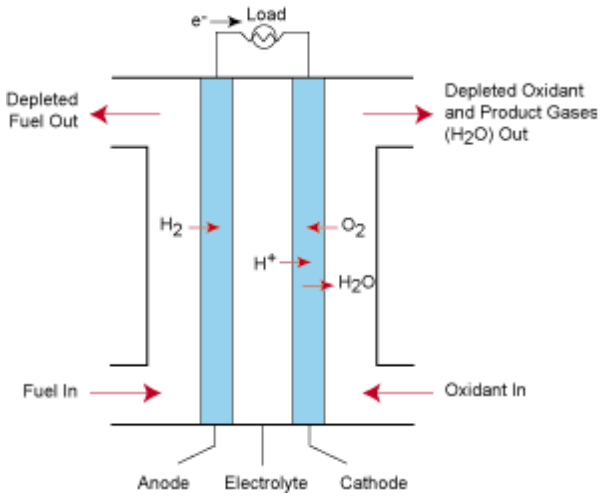

Figure 1.2 PEM Fuel cell Operation [2].

The reactions taking place in PEMFC are

Anode: $H_2 \rightarrow 2H^+ + 2e^-$

Cathode: $\frac{1}{2} O_2 + 2H^+ + 2e^- \rightarrow H_2O$

Overall: $H_2 + \frac{1}{2} O_2 \rightarrow H_2O$

PEM Fuel cells have high power density hence preferred for automotive applications. The use of a solid electrolyte lowers the corrosion taking place and requires no liquid

management. It has a low operating temperature between 70-90 degrees C. This makes it start quickly and suitable for automotive applications. They have longer life and are maintenance free. This uses platinum as a catalyst which increases cost of the fuel cell and is also sensitive to carbon monoxide [2].

1.5 PEM Fuel Cell's History

Fuel cells were invented in 1839.PEM technology was developed in early 1960s for U.S Navy and Army. The next development in PEM was for NASA's project Gemini in early days of the U.S piloted space program. By mid 1970's PEM cells were developed for under water life support leading to U.S Navy oxygen generating fleet [3].

PEM fuel cells started in space but can be used in stationary and portable applications including lighting, communications, navigation, computation and entertainment. Vehicular applications include buses, long distance aircraft and cars.

Current Status of PEM Fuel cells [4]

1. Commercial products for back up power are available (30kw)
2. Specialty vehicle and portable power products are pre-commercial (< 85kw)
3. Commercially available direct hydrogen PEM Fuel Cell Modules for specialty vehicles are given in the table (I) below.

Table I Commercially available direct Hydrogen PEM Fuel Cell Modules for Specialty Vehicles

Manufacturer	Application	Size
Ballard	Light duty vehicle applications	4kw, 8.8kw, 13.2kw, 19.3kw, 85kw
Hydrogenics	Commercial vans, transit buses, neighborhood electric vehicles	8.5kw, 15kw, 17kw, 66kw
Nuvera	Industrial vehicles and equipment	5kw

4. Toyota has developed a PEM fuel cell of 90kW. The type of the motor is synchronous permanent magnet which can deliver a maximum output of 80kW and maximum torque of 260n-m and the secondary battery is nickel metal hydride.
5. Ballard has developed a PEM fuel cell of 78kW.The AC synchronous motor is used and it delivers a maximum output of 60kW and maximum torque of 272n-m. The secondary battery is ultra capacitor.
6. General Motors has developed a PEM fuel cell of 94kW with 440 series connected cells. Synchronous permanent magnet motor delivers a maximum output of 60kW and maximum torque of 215n-m. The secondary battery used is nickel metal hydride.

PEM fuel cell modules are currently available; currently no PEM fuel cell integrated specialty vehicle products are commercially available. Numerous products are in testing and it is anticipated that commercial will be available soon. Also, many PEM fuel cell modules are available but currently they are not commercially available. Numerous products are in testing and it is anticipated that they will be commercially available in the near future.

1.6 Organization of the Report

Chapter 2 explains the PEM fuel cell mathematical modeling and basic equations involved in its operation .It presents the simulink model of PEM fuel cell and the equivalent model. Also the results of the PEM model have been presented in the form of graphs.

Chapter 3 gives the detail description and design methodology of the energy storage unit and explains the energy storage unit's role in fuel cell hybridization. The optimized combination of battery and ultra capacitor is explained .Also the DC-DC converters used for interfacing are presented. This chapter discusses the simulations and results for the energy storage unit model and the parallel model where the energy storage unit and the PEM cell are connected in parallel such that they share the same load. The results are presented in form of graphs obtained from the simulation of the models.

Chapter 4 concludes the report by summarizing the work and providing suggestions for any future work.

Chapter 2

PEM FUEL CELL MODEL

A PEM fuel cell is being investigated as an alternative source of power for automotive applications like cars and buses. To emulate the fuel cell characteristics for optimizing its performance and develop fuel cell power converters for various applications a Simulink model has been presented. The ohmic, polarization and activation losses, double layer charging effect and thermodynamic characteristics inside the fuel cell are included in the model. The static and dynamic characteristics are obtained through simulation.

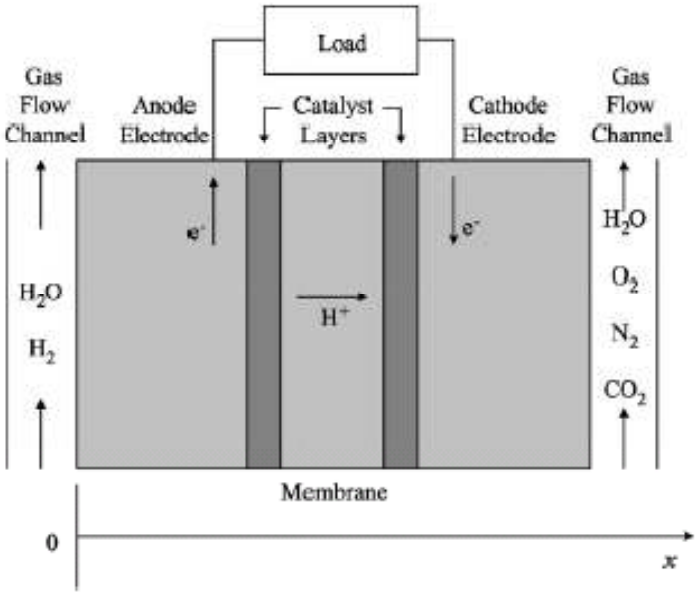

Figure 2.1 PEM Fuel Cell Stack [6].

The model includes all the important characteristics of a fuel cell stack. The dynamic models are presented using electrical circuits. Initially the equivalent internal voltage source and equivalent resistors for activation, ohmic and concentration losses are assessed using mechanistic analysis. Then, the double layer charging effect is considered by adding an equivalent capacitor to the circuit. The thermodynamic characteristic inside the fuel cell is also integrated into the model according to the energy balance equation. The impact variables pressure, temperature and gas constituents on fuel cell performance are also assessed [6].

2.1 Gas Diffusion in the Electrodes

In order to calculate the fuel-cell output voltage we need the partial pressures of H_2 and O_2.

The partial pressures of reactants are [5]:

$P_{Anode} = P_{H2} + P_{H2O}$

$P_{Cathode} = P_{O2} + P_{H2O} + P_{N2} + P_{CO2}$

The fuel supply (anode gas) is composed of hydrogen and water vapor and the air supply (cathode gas) is composed of oxygen, N_2, CO_2 from air and water vapor.

In a gas mixture consisting of N species, the diffusion of component i through the porous electrodes can be described by the Stefan Maxwell formulation [6].

$$\Delta x_i = \frac{RT}{P} \sum_{j=1}^{N} \frac{x_j N_j - x_j N_i}{D_{ij}} \quad (1)$$

Where x_i is the mole fraction of the species i

R: Gas constant, 8.3143 J/ (mol.k)

T: Temperature in Kelvin

N_i: Superficial gas flux of species i [mol/(m^2.s)]

$D_{i,j}$: Diffusivity (Effective binary Diff) of i-j pair [m^2/s]

P: Pressure (Pascals)

The anode channel has a gas stream mixture of H_2 and H_2O (g).The major flux of water (in gas phase) normal to anode surface N_{H2O} can be set to zero according to assumptions.

1) One dimensional treatment.
2) Ideal and uniformly distributed gases.
3) Constant pressures in the fuel cell gas flow channels.

In one dimensional (1-D) transport process along the x axis the diffusion of water can be simplified as

$$\frac{dx_{H20}}{dx} = \frac{RT}{P_a}\left(\frac{x_{H20}N_{H2} - x_{H2}N_{H20}}{D_{H20,H2}}\right) \quad (2)$$

The molar flux of H_2 can be determined by Faradays law.

$$N_{H2} = \frac{I_{den}}{2F} \quad (3)$$

Combining (2) and (3) and integrating with respect to x from anode channel to catalyst surface it gives

$$x^*_{H20} = x^{channel}_{H20} \exp\left(\frac{RTI_{den}l_a}{2FP_aD_{H20H2}}\right) \quad (4)$$

I_{den} : Current density (A/m^2)

L_a : Width between anode channel to catalyst (m)

F: Faraday Constant (96487 coulombs per mol)

Since $x^*_{H2O} + x^*_{H2} = 1$, the effective partial pressure of H_2 is

$$p^*_{H_2} = \frac{p^*_{H20}}{x^*_{H20}}(1 - x^*_{H20}) \quad (5)$$

According to the consideration that as fuel is humidified H_2 and oxidant is humidified air we assume anode water vapor pressure is 50% of the saturated vapor pressure while the effective cathode vapor pressure is 100%.

$$p^*_{H_2} = 0.5p^{sat}_{H20}\left[\frac{1}{x^{channel}_{H20}\exp\left(\frac{RTI_{den}l_a}{2FP_aD_{H20H2}}\right)} - 1\right] \quad (6)$$

The gases flowing in cathode channel are O_2, N_2 and H_2O (g) and CO_2. Using (1) the diffusion of H2O (g) at cathode side can be obtained from

$$\frac{dx_{H20}}{dx} = \frac{RT}{P_c}\left(\frac{x_{02}N_{H20} - x_{H20}N_{02}}{D_{H20,02}}\right)$$

$$= \frac{RT}{P_c}\left(\frac{-x_{H20}N_{02}}{D_{H20,02}}\right) \quad (7)$$

$$x^{*}_{H20} = x^{channel}_{H20} \exp\left(\frac{RTI_{den} l_c}{2FP_c D_{H20,H2}}\right) \quad (8)$$

L_c : Width between cathode channel to catalyst (mt).

Similarly,

$$x^{*}_{N2} = x^{channel}_{N2} \exp\left(\frac{RTI_{den} l_c}{4FP_c D_{N2,o2}}\right) \quad (9)$$

$$x^{*}_{CO2} = x^{channel}_{CO2} \exp\left(\frac{RTI_{den} l_c}{4FP_c D_{CO2,o2}}\right) \quad (10)$$

The effective mole fraction of O_2 is

$$x^{*}_{O2} = 1 - x^{*}_{H2O} - x^{*}_{N2} - x^{*}_{C02} \quad (11)$$

The corresponding partial pressure of O_2 is

$$p^{*}_{O2} = \frac{p^{*}_{H20}}{x^{*}_{H20}} x^{*}_{O2}(1 - x^{*}_{O2} - x^{*}_{N2} - x^{*}_{CO2}) \quad (12)$$

Also, $P^{sat}_{H2O} = P^{*}_{H2O\ Hence}$

$$p^{*}_{O2} = p^{sat}_{H20}\left[\frac{1 - x^{*}_{N2} - x^{*}_{CO2}}{x^{*}_{H2O}} - 1\right] \quad (13)$$

2.2 Material Conservation Equations

$$\frac{V_a}{RT}\frac{dp^{*}_{H2}}{dt} = M_{H2,in} - M_{H2,out} - \frac{i}{2F}$$

$$= M_{H2,net} - \frac{i}{2F} \quad (14)$$

This is the instantaneous change in effective partial pressures of Hydrogen.

Similarly Instantaneous change in effective partial pressure of oxygen is

$$\frac{V_c}{RT}\frac{dp^{*}_{O2}}{dt} = M_{O2,in} - M_{02,out} - \frac{i}{4F}$$

$$= M_{02,net} - \frac{i}{4F} \quad (15)$$

At steady state partial pressures are constant hence

$$\frac{dp^{*}_{H2}}{dt} = \frac{dp^{*}_{O2}}{dt} = 0 \quad (16)$$

Therefore,

$$M_{H2,\,net} = 2M_{02,\,net} = \frac{I}{2F} \qquad (17)$$

Under transient state, there are delays between changes in load current and flow of fuel and oxidant. The following relationships are used to represent these delay effects [6].

τ_a : Fuel flow delay (in sec)

τ_c : Oxidant flow delay (in sec)

$$\tau_a \frac{dM_{H2,\,net}}{dt} = \frac{i}{2F} - M_{H2,\,net}$$

$$\tau_c \frac{dM_{O2,\,net}}{dt} = \frac{i}{4F} - M_{O2,\,net} \qquad (18)$$

2.3 Fuel Cell Output Voltage

The overall reaction in the PEM fuel cell can be expressed as

$$H_2 + \frac{1}{2}O_2 = H_2O_{(l)} \qquad (19)$$

We assume fuel cell works less than 100 degrees C and reaction product is in liquid phase. The corresponding Nernst equation is used to calculate the Reversible potential. The Nernst equation provides a relation between the ideal standard potential (E^0) for the cell reaction and ideal equilibrium potential (E) at other temperatures and partial pressures of reactants and products. According to Nernst equation ideal cell potential at given temperature can be increased by operating at higher reactant pressures and improvements in fuel cell performance have been observed at higher pressures [6].

$$E_{cell} = E_{o,\,cell} + \frac{RT}{2F} \ln [p^*_{H2} \cdot (p^*_{O2})^{0.5}] \qquad (20)$$

E: Reversible potential of each cell (in volts)

E_0 : Reference potential (in volts)

E^0: Standard reference potential (in volts)

$E_{0,\,cell}$ is the function of temperature and can be expressed as

$$E_{o,\,cell} = E^{o}{}_{o,\,cell} - k_E(T - 298) \qquad (21)$$

Where $E^{o}{}_{o,\,cell}$ is standard reference potential at standard state, 298k and 1atm pressure.

k_E is the empirical constant in calculating E_0 (in volts per Kelvin).

A voltage $E_{d,\,cell}$ is considered to be subtracted from the right side of (20) for the overall effect of the fuel and oxidant delay.

The steady state value $E_{d,\,cell}$ is zero but it will show influence of fuel and oxidant delays on the fuel cell output voltage during load transients.

$$E_{d,\,cell} = \lambda_e[i(t) - i(t)\exp\left(-\frac{t}{\tau_e}\right) \qquad (22)$$

τ_e : Overall Flow delay (in sec)

λ_e: Constant factor in calculating E_d [Ω]

Hence Converting (22) to Laplace domain

$$E_{d,\,cell}(s) = \lambda_e I(s)\frac{s\tau_e}{(s\tau_e+1)} \qquad (23)$$

Hence the internal potential E_{cell} becomes

$$E_{cell} = E_{o,\,cell} + \frac{RT}{2F}\ln[p^*_{H2}\cdot(p^*_{O2})^{0.5}] - E_{d,\,cell} \qquad (24)$$

Under normal operating conditions fuel cell output voltage is less than E_{cell} due to ohmic, concentration and activation losses.

Hence,

$$V_{cell} = E_{cell} - V_{act,\,cell} - V_{ohm,\,cell} - V_{conc,\,cell} \qquad (25)$$

Hence,

$$V_{out} = N_{cell}E_{cell} = E - V_{act} - V_{ohm} - V_{conc} \qquad (26)$$

2.4 Activation, Ohmic and Concentration Losses

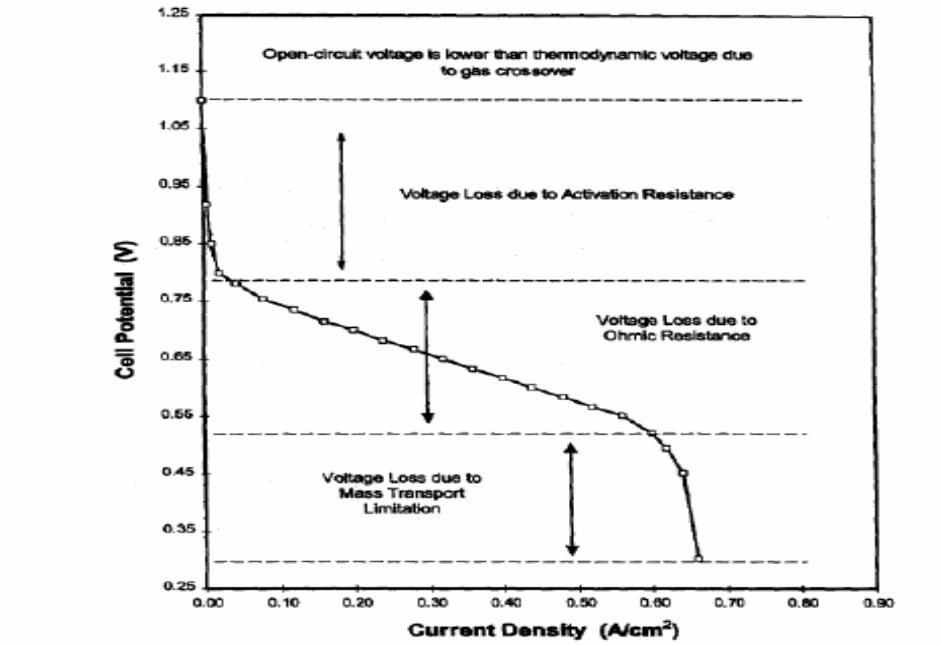

Figure 2.2 Typical Polarization Curve [7].

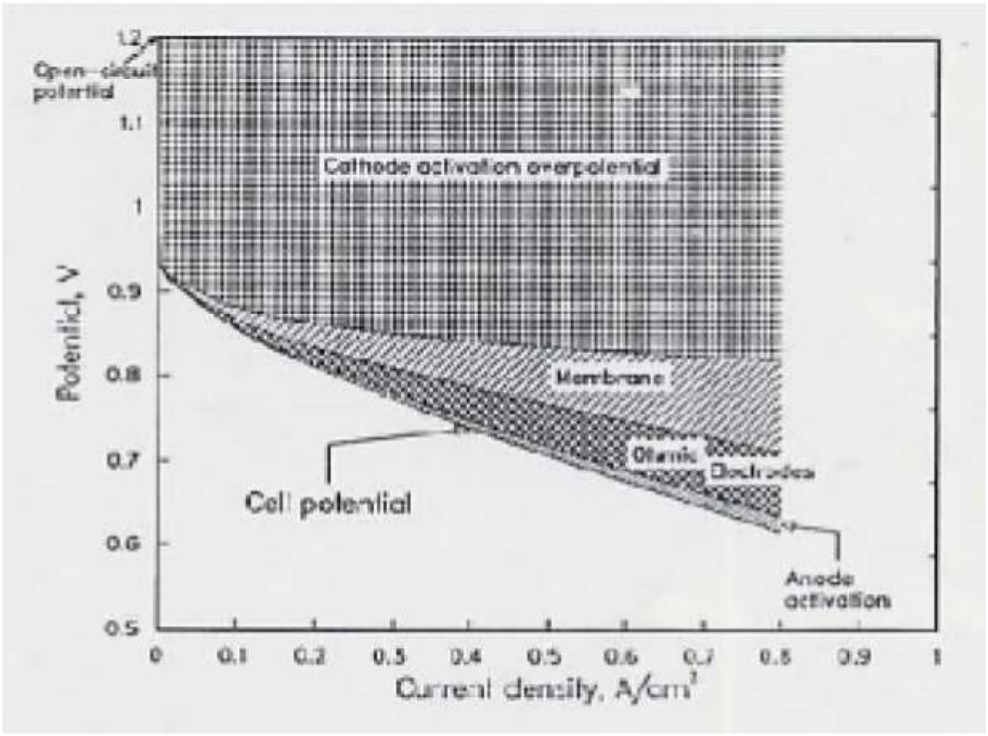

Figure2.3 Typical Losses in PEM Fuel Cell [7].

2.4.1 Activation Voltage Drop

Activation voltage drop is dominant at low current density. At this point electronic barriers have to be overcome prior to current and ion flow. Active polarization is produced because of the energy intensity activity of making and breaking of chemical bonds at anode and cathode. At anode fuel enters a reaction site and is broken into ions and electrons through the use of catalyst. The resulting ions form the bonds with catalyst surface while the other electrons remain near the ions until another fuel molecule begins to react with the catalyst, thus breaking the bond with the ion. The energy input to break the bond with the ion determines whether the electron will bond again with the ion, or will remain separate. The electron migrates through the bipolar plate while ion diffuses through the catalyst [8].

The same procedure occurs at cathode. Incoming oxygen is broken up into components by the catalyst where it draws electrons, ions and oxygen atom together to form water that is taken from electrode and ejected into the gas channel and out of the cell.

The amount of energy needed for forming and destroying of these bonds comes from the fuel and reduces the overall energy the cell can produce. The reduction is controlled by the reaction rate of the cell. If the reaction rate increases the flow rate for the fuel must increase which increases the kinetic energy and thus lowers energy required to break the bonds.

Increasing temperature, active area of the electrode and utilization of the catalyst also lowers the effect of active polarization. The activation losses can be obtained by Tafel equation [6].

$$V_{act} = \frac{RT}{\propto zF} \ln\left(\frac{I}{I_0}\right) = T.\,[a+b.\ln(I)] \quad (27)$$

$$V_{act} = \eta_o + (T - 298).a + T.b.\ln(I) = V_{act1} + V_{act2} \quad (28)$$

Where $V_{act1} = \eta_0 + (T\text{-}298).a$ is the voltage drop effected only by the fuel cell internal temperature, while $V_{act2} = (T.b.\ln(I))$ is both current and temperature dependent.

$$R_{act} = V_{act2}/I = (T.b.\ln(I))/I \quad (29)$$

2.4.2 Ohmic Polarization

Ohmic polarization is caused by electric losses in the cell. The resistances of the current collecting plates, electrodes and electrolyte are all factors which add to the energy loss.

$V_{ohm} = V_{ohm,\,a} + V_{ohm,\,membrane} + V_{ohm,\,c} = IR_{ohm}$ (30)

The ohmic resistance of a PEM Fuel cell consists of the resistance of polymer membrane, the conducting resistance between the membrane and electrodes and the resistances of the electrodes.

R_{ohm} is the function of current and temperature.

Where $R_{ohm} = R_{ohm\,0} + k_{RI}\,I - k_{RT}\,T$ (31)

$R_{ohm\,0}$ is the constant part of Rohm, k_{RI} is empirical constant in calculating R_{ohmic} [Ω/A] and k_{RT} is empirical constant in calculating R_{ohmic} [Ω/K].

2.4.3 Concentration Polarization

During the reaction process there would be restriction to transport the fuel gases to reaction sites. This usually occurs at high current because the forming of product water and excess humidification blocks the reaction sites. This polarization is also affected by the physical restriction of the transfer of a large atom, oxygen to the reaction sites on the cathode side of the fuel cell. It can be reduced by increasing the gas pressure which drives water out of the cell and increases fuel concentration using high surface area electrodes or using thinner electrodes which shortens the path of gas to the sites.

$$V_{conc} = -\frac{RT}{zF}\ln\frac{C_S}{C_B} \quad (32)$$

Where Z is number of electrons involved in the reaction, C_S is surface concentration and C_B is bulk concentration.

According to Fick's First law and Faraday's law the above equation can be rewritten as

$$V_{conc} = -\frac{RT}{zF}\ln\left(1 - \frac{I}{I_{limit}}\right) \quad (33)$$

The equivalent resistance for concentration loss is

$$R_{conc} = \frac{V_{conc}}{I} = -\frac{RT}{zFI}\ln\left(1 - \frac{I}{I_{limit}}\right) \quad (34)$$

2.4.4 Double Layer Charging Effect

In a PEM fuel cell, two electrodes are separated by a solid polymer membrane which allows only H+ ions to pass but blocks electron flow. The electrons will flow from external load and gather at the surface of cathode to which protons of hydrogen will be attracted at the same time. Thus, two charged layers of opposite polarity are formed across the boundary between the porous cathode and the membrane [6]. The layers known as electrochemical double layer can

store electrical energy and behave like a super capacitor. The equivalent circuit of the fuel cell considering this effect is given in the below figure.

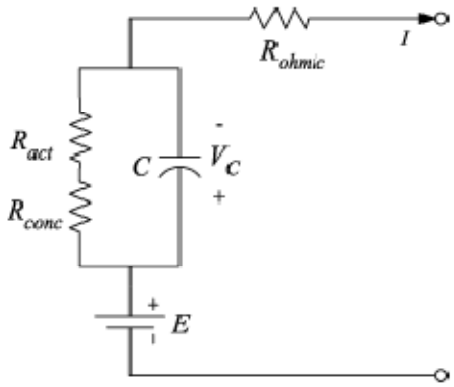

Figure 2.4 Double Layer Charging Effect [6].

C is equivalent capacitor due to the double layer charging effect. Since the electrodes of a PEM fuel cell are porous the capacitance, C is very large and can be in order of several farads.

$$V_C = (I - C\frac{dV_c}{dt})(R_{act} + R_{conc.}) \quad (35)$$

The double layer charging effect is integrated into the modeling by using V_C instead of V_{act2} and V_{conc} to calculate V_{out}. Now the fuel cell output voltage turns to be

$$V_{out1} = E - V_C - V_{act1} - V_{ohm} \quad (36)$$

2.5 Energy Balance of Thermo Dynamics

The net heat generated by the chemical reaction inside the fuel cell which causes temperature to rise or fall, can be written as

$$\dot{q}_{net} = \dot{q}_{chemical} - \dot{q}_{electrical} - \dot{q}_{sens+latent} - \dot{q}_{loss} \quad (37)$$

where q_{net} is net heat energy (Joules), $q_{sens + latent}$ is sensible and latent heat (in joules).

The available power released due to chemical reaction is calculated by

$$\dot{q}_{chemical} = \dot{n}_{H_2,\,consumed} \cdot \Delta G \quad (38)$$

ΔG is Gibbs free energy which changes with temperature as follows

$$\Delta G = \Delta G_o - RT\ln[p^*_{H2}.(p^*_{O2})^{0.5}] \quad (39)$$

2.5.1 Gibbs Free Energy

Potential can also be expressed in Gibbs free energy. Gibbs free energy is the maximum amount of mechanical work which can be obtained form given quantity of a certain substance in a given initial state without increasing the total volume or allowing heat to pass to or from external bodies.

When a system changes from well defined initial state to final state Gibbs free energy ΔG equals to work exchanged by the system with its surroundings less the work of the pressure forces during reversible transformation of system from same initial state to final state. It is also chemical potential that is minimized when system reaches equilibrium at constant pressure.

The electric output power is computed as

$$\dot{q}_{electrical} = V_{out}.\ I \quad (40)$$

The sensible and latent heat absorbed during the process can be estimated by

$$\dot{q}_{sens+latent} = (\dot{n}_{H_2,\ out}.\ T - \dot{n}_{H_2,\ in}.\ T_{room}).\ C_{H_2}$$

$$+ (\dot{n}_{O_2,\ out}.\ T - \dot{n}_{O_2,\ in}.\ T_{room}).\ C_{O_2}$$

$$+ \dot{n}_{H_2O,\ generated}.\ (T - T_{room}).\ C_{H_2O,l} + \dot{n}_{H_2O,\ generated}.H_V \quad (41)$$

Where T_{room} is the room temperature,

C_i is the specific heat capacity of species I [J/ (mol.k)]

H_v is vaporization heat of water (joules/mol)

The heat loss which is mainly transferred by air convention can be estimated by following formula

$$\dot{q}_{loss} = h_{cell}\,(T - T_{room})\,N_{cell}A_{cell} \qquad (42)$$

Where h_{cell} is convective heat transfer coefficient [W/ (m^2/s)]

N_{cell} is number of cells and A_{cell} is area of each cell [m^2]

At steady state $\dot{q}_{net} = 0$ and fuel cells operates at some constant temperature. During transitions the temperature of fuel cell will drop or rise according to the following equation

$$M_{FC}C_{FC}\,(dT/dt) = \dot{q}_{net} \qquad (43)$$

Where M_{FC} is total mass of fuel cell stack and C_{FC} is overall specific heat capacity of stack.

2.6 Simulink Model

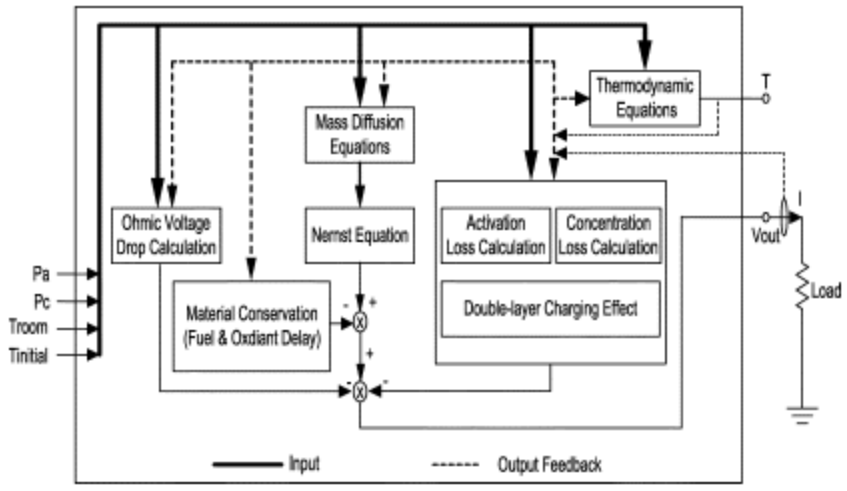

Figure 2.5 Simulink Model of the PEM Fuel Cell [6].

The fuel cell output voltage, which is a function of temperature and load current,can be obtained from the above model (Figure 2.5).The input quantities are Pa, Pc, Troom and Tinitial. At any given load current, time, the internal temperature T is determined and both load current and temperature are fed back to different block which take part in calculation of V_{out}[6].

2.6.1 Steady State Responses of the PEM Fuel Cell

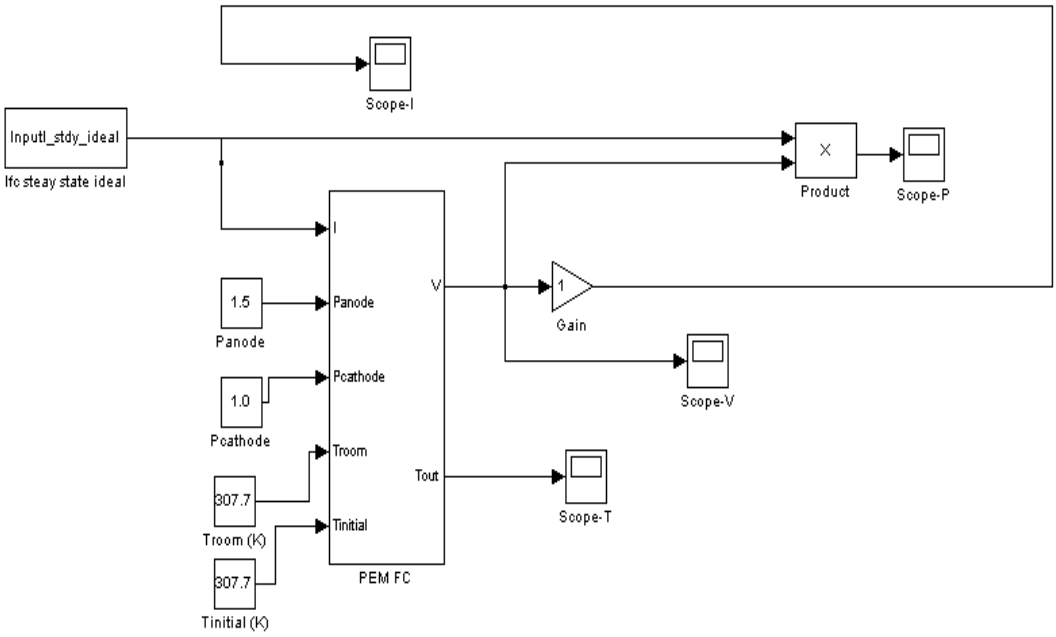

Figure 2.6 Schematic of the PEM Fuel Cell in Simulink.

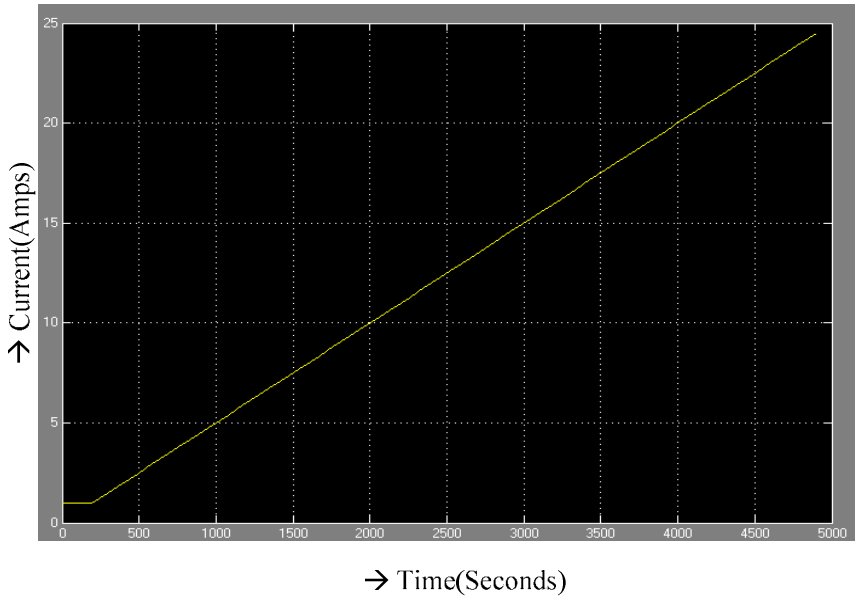

Figure 2.7 Load Current of the PEM Fuel Cell.

Peak output power occurs near fuel cell rated output beyond which fuel cell goes into the concentration zone. In this region fuel cell output power will decrease with increasing load current due to sharp decrease in terminal voltage.

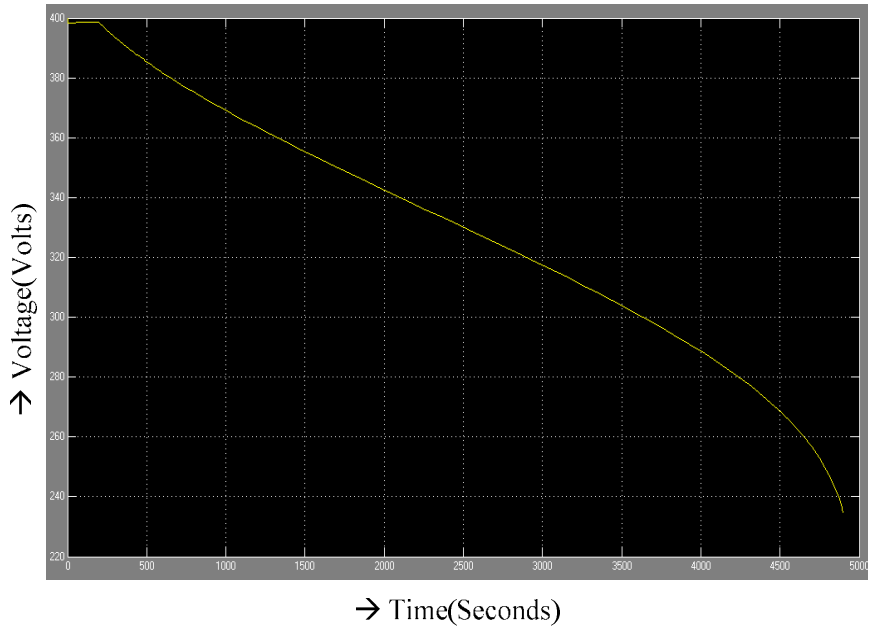

Figure 2.8 Voltage Curve of the PEM Fuel Cell.

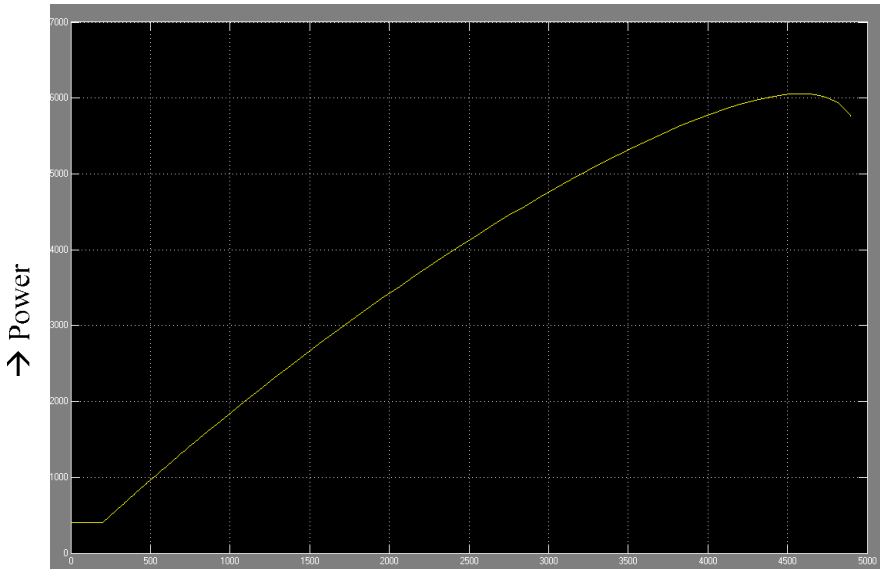

Figure 2.9 Power curve of the PEM Fuel Cell.

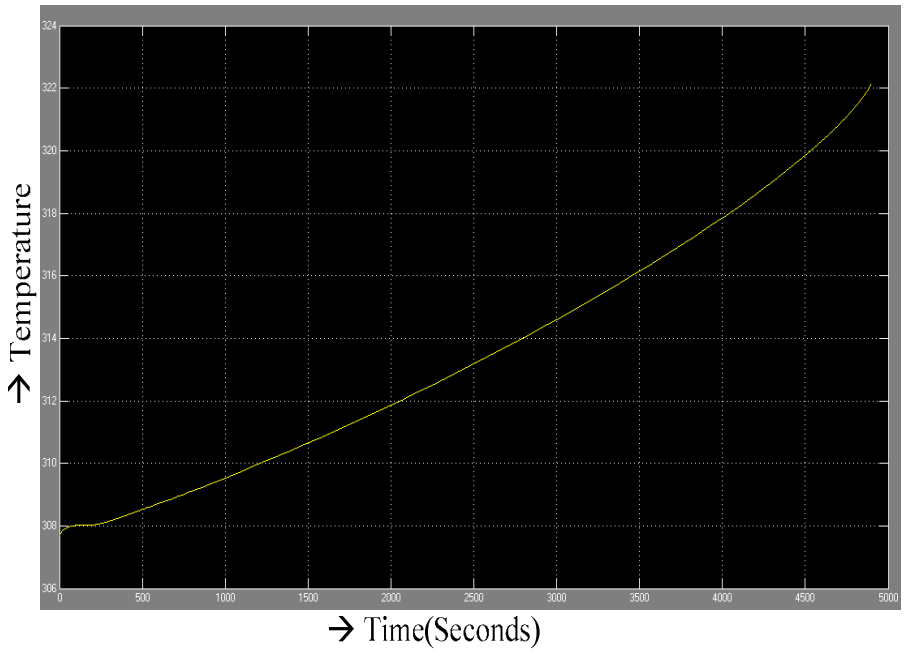

Figure 2.10 Temperature Response of the PEM Fuel Cell.

The above graphs (Figures 2.7, 2.8, 2.9 and 2.10 represent the steady state responses of a PEM fuel cell obtained through the simulations. All the responses are similar to the results obtained in [6].

2.6.2 Transient Performance

The dynamic property of PEM fuel cell depends mainly on double layer charging effects, fuel and oxidant flow delays and thermodynamic characteristics inside the fuel cell.

Although C is large, time constant T = (R_{act} +R_{conc}).C is small because (R_{actv}+R_{conc}) is small when fuel cell works in linear zone. Therefore C affects transient response in short time range. When load current steps up voltage drops simultaneously to some value due to voltage drop across R_{ohm} and then it decays exponentially to its steady state due to capacitance double layer charging effect.

The fuel and oxidant flows cannot follow the load current change instantaneously. Also temperature of fuel cell stack cannot change instantaneously.

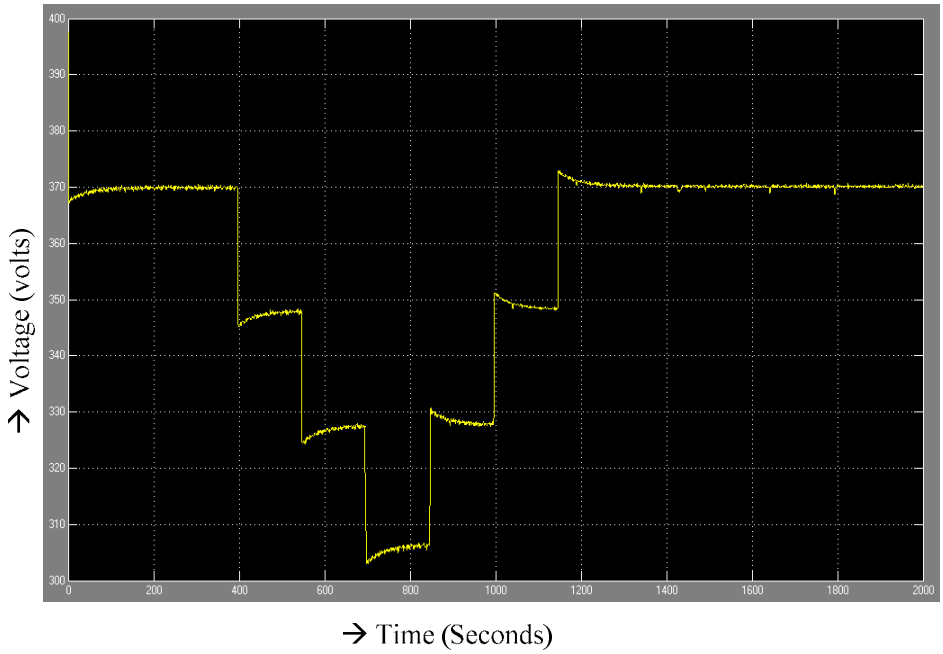

Figure 2.11 Transient Response of a PEM Fuel Cell.

The above graph (Figure 2.11) represents the transient response of a PEM fuel cell obtained through simulation. All the responses are similar to the results obtained in [6].

2.6.3 Output Voltage of the PEM Fuel Cell with Variable Step Load Current

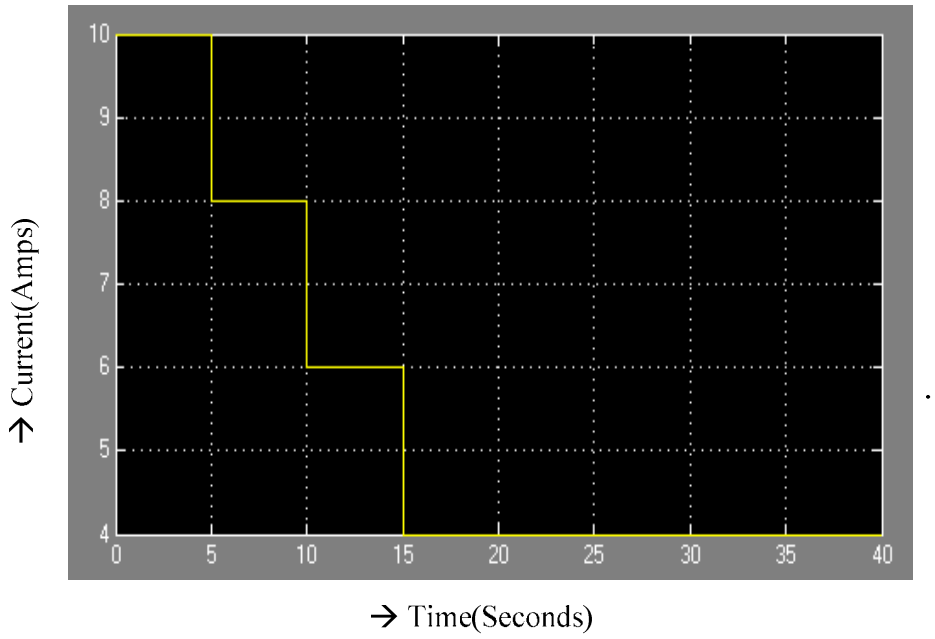

Figure 2.12 Variable step Load Current.

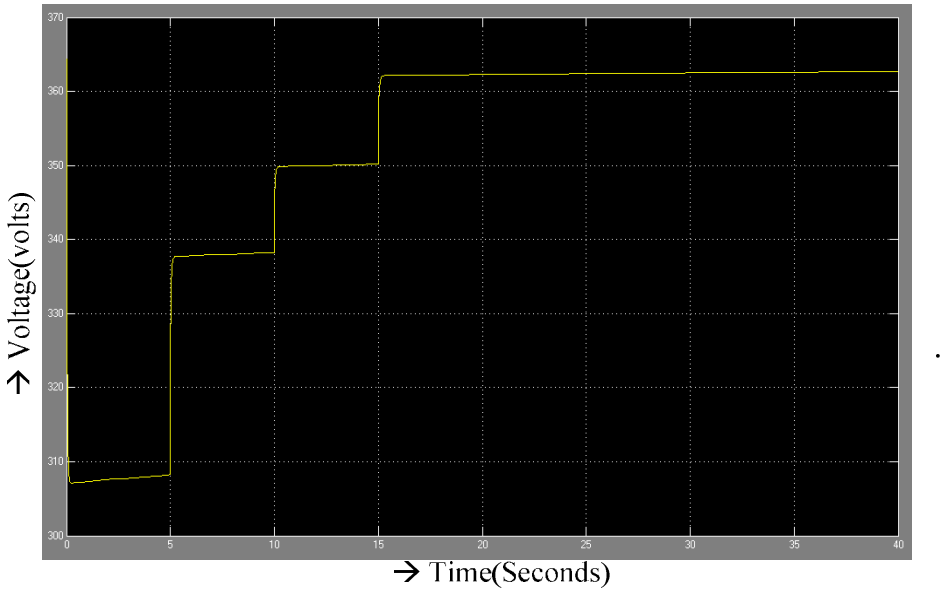

Figure 2.13 Output voltage of the PEM Fuel Cell.

From the above graph (Figure 2.13) it can be clearly seen that the output voltage follows the load current.

Chapter 3

ENERGY STORAGE UNIT

Vehicle hybridization with electrochemical energy storage technologies including lead-acid, nickel-metal hydride, lithium ion and ultra capacitors could provide an alternative path to break the current barriers to fuel cell applications. Pure fuel cell has a bad acceleration performance and cannot make use of the braking energy and hence due to fuel cell's inability for energy regeneration fuel economy and driving range cannot be improved. Hybridizing fuel cell vehicles can have several benefits including capturing regenerative breaking energy, enhancing fuel economy, providing a more flexible operating strategy overcoming fuel cell cold-start, transient short falls and lowering the cost per unit power [10]. Thus it is beneficial to have a hybrid vehicle in which fuel system supplies base power while battery and ultra capacitor supplies peak power for fast acceleration and captures braking for regeneration. This chapter discusses the energy storage requirements of a vehicle which helps in determining the power rating of main energy source and auxiliary storage unit for a mid size SUV. The design methodology stated in [11] has been followed.

3.1 Energy Storage Unit's (ESU's) role in Fuel Cell Hybridization

3.1.1 Traction Power during Fuel Cell Start up

To be capable of start and go driving all propulsion power components must be operational shortly after the driver turn the key. For fuel vehicles with an on-board fuel processor must produce and deliver sufficient hydrogen to the fuel cell on this basis. This requirement is relaxed in a hybrid vehicle operated by fuel cell and battery, since battery can provide initial traction power while fuel cell system warms up to its operating temperatures.

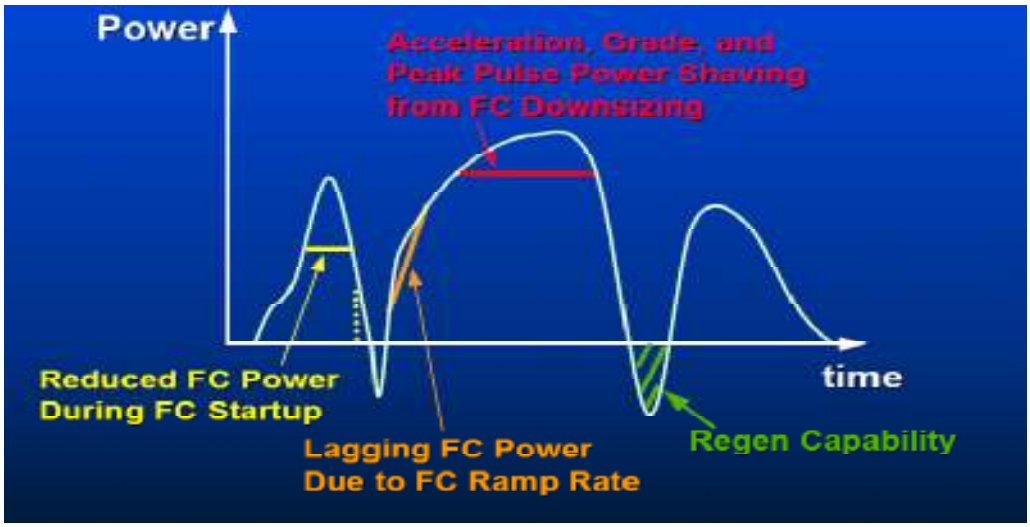

Figure 3.1 Pictorial Description of roles of Energy Storage Unit [9].

Under ambient and cold start conditions it is likely that fuel cell system power output is less than its rated power. The reduction in the power output capability from rated power at 80c could be as large as 50% when the system has been kept at 20c based on model predictions. In some configurations energy storage system will be expected to compensate for the limited fuel cell system performance.

3.1.2 Power assist during Drive Cycles

The energy storage unit can provide the power assist capability in multiple ways. It can perform peak shaving. If the fuel cell system rated power has been reduced such that the drive cycle loads are greater than its capability, the energy storage unit can provide power during these transient peak power events. Also, it can improve the transient response of the traction system when fuel cell is not capable of responding quickly to an increase in power.

3.1.3 Regenerative Braking Analysis

The Regenerative energy dissipated at friction brakes should be collected by the energy storage unit.

However, these requirements do not necessarily lead us to correct balance between a fuel cell size and battery pack size. Hence it is useful to consider the peak power and energy requirements encountered on acceleration and grade performance tests.

3.1.4 Acceleration and Grade Performance Requirements

During acceleration the Energy Storage unit can be used for traction assistance. When the fuel cell is downsized the energy storage unit can provide the traction assist during high power transients to meet the drive cycle requirements.

The long term gradeability requirement may lead to a significantly large energy storage unit. Hence generally ESU would provide only minimal contribution to the grade performance and hence the minimum fuel cell system size should correlate to the power required to provide continuous grade performance capability.

3.1.5 Electrical Accessory Loads

The electrical accessory loads in a fuel cell hybrid vehicle may include radiator fans, electric power steering, electric brakes, air conditioning systems etc. In general these loads will vary throughout the drive cycle, but the net effect can be accounted for by applying a constant average accessory load over the duration of the drive cycle. In a fuel cell hybrid vehicle battery could potentially be expected to maintain the electrical accessory loads for periods during the cycles. The ESU must have power and energy capacity to support these loads when the fuel cell is shut down if start/stop hybrid operation is allowed. However over the long run the fuel cell would need to provide the bulk energy to support the accessory loads.

3.1.6 Fuel Cell System Start-up and Shut down

In hybrid fuel cell vehicle it would be desirable to be able to have start/stop capability. This means that while the vehicle is operating, the fuel cell can be shut down and restarted on as needed basis. Shutting down the system under low power demand scenarios can save a significant amount of fuel. The energy storage requirements will not be included in this report.

3.1.7 Cost and packaging considerations

The total system cost can drive the final system design requirements for production vehicles. The cost per kW of the fuel cell is extremely high but is expected to drop dramatically in long term. Most energy storage technologies are less expensive than the fuel cell systems on a per kW basis today. Therefore from the cost perspective it would be reasonably expected that a system with large battery and small fuel cell would be logical today.

3.2 Design Methodology of the ESU

The design methodology is for a combined Battery-Ultracapacitor energy storage unit. The model of the half-bridge converter is used in the battery Ultracapacitor ESU. Simulink is used to obtain the results. This methodology presents ESU used for power management of loads with large peak-to-peak average power ratios such as mid size Sport Utility Vehicle (SUV). The power management can be illustrated by the following figure.

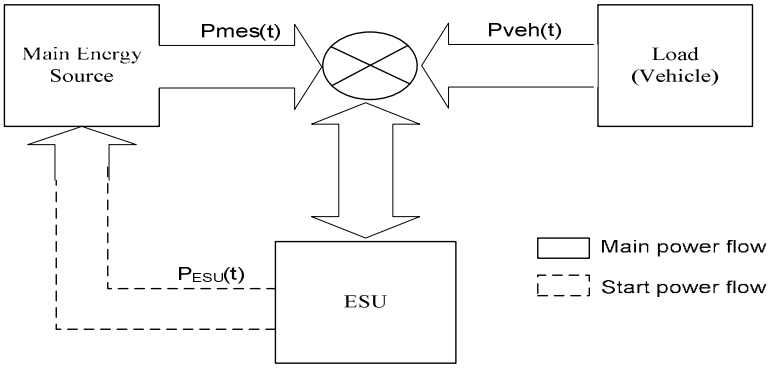

Figure 3.2 Diagram of Power Management System.

The power management concept is based on storing and releasing power $P_{ESU}(t)$ from an ESU to instantaneously match the vehicle power generation $P_{mes}(t)$, to the vehicle power demand, $P_{veh}(t)$, without having to instantaneously change the main energy source[11].Instantaneous power requirement, $P_{ESU}(t)$ can be determined by subtracting the instantaneous power requirement, $P_{veh}(t)$ of the load from the instantaneous power, $P_{mes}(t)$ provided by the main energy source.

3.3 Load Requirements

The vehicle instantaneous power requirement, $P_{veh}(t)$ can be estimated using simplified dynamic equation or simulation such as advisor using physical dimensions weight and driving schedules for a given vehicle[11].

Table II Mid Size SUV Physical Dimensions

Parameter	Value
Rolling Coefficient	0.012
Aero dynamic drag coefficient	0.44
Frontal Area	2.66 m^2
Glider Weight	1200 kg
Engine weight	500kg
Transmission weight	150kg
Curb weight	1850kg
Gross weight	2350kg

Table III Mid Size SUV Performance Requirements

Parameter	Value
Maximum Velocity	100mph
Rated Velocity	85mph
Acceleration[0-60mph]	<11.0s
Acceleration[40-60mph]	<5s
Acceleration[0-85mph]	<21s
Maximum Acceleration	4.3m/s^2
Gradeability at 55mph during 20min	6%
Payload Capacity	500kg
Towing(Min/Max)	500/3000kg

Table IV SUV Power and Energy Requirements

Driving Schedule or Condition	Peak Power(kW)	Average Power(kW)	Energy[kJ]
Z60 in 10.0s	150.0	150.0	416.6
Acc. 40-60mph in 5s	150.0	150.0	208.3
Z85 in 21 s	150.0	150.0	875.0
C85 0% grade	53.8	53.8	--
C55 6% grade	64.5	64.5	--
UDDS	59.4	6.3	8.664
HWFET	48.4	16.4	12,547
NEDC	62.6	6.8	8,132
Japan 10-15	34.1	4.2	2,765

The parameters listed in the above table III are typical driving schedules and their corresponding power requirements. Z60 in 10s is 0 mph to 60 mph in 10 seconds. Acc. 40-60 mph in 5s is 40 mph to 60 mph in 5 seconds. Z85 in 21 s is 0 mph to 85 mph in 21s. C85 0% grade is constant speed of 85 mph at 0% grade.C55 6% grade is constant speed of 55 mph at 6% grade UDDS is urban dynamometer driving schedule, representing typical urban driving and is part of US EPA federal test procedure. HWFET is high speed moderate acceleration rate driving profile. NEDS is the new European drive cycle. Japan 10-15 is the Japanese model cycle, characteristic of congested driving in a Japanese city. The values here are calculated using advisor.

3.3.1. Main Energy Source [11]

The first step is determining the rated power of the main energy source. From Table IV, it is 150kW without using an ESU. However, this power is required only for a short period of time (normally less than 30 seconds) [11].

The concept of power management assumes that main energy source provides the average power or steady state power while ESU provides peak or transient power. Thus a time constant must be defined to differentiate between steady state and transient operation.

For SUV, one could assume that the main energy source, the fuel cell achieves 90% of its rated power within 2 seconds. Any power requirement over 2 seconds is considered steady state. In this case rated power of the main power source must be 150kW and this system will not require an ESU. Now, if a power requirement over 30sec is considered steady state , the main source rated power could be reduced to 64.5kW which is the power required to maintain 55mph in 6%grade for 20minutes.This power is greater than power to maintain rated speed at 0% grade. The difference must be provided by ESU. The rated power of 64.5kW could be increased by a predetermined safety factor. The power is increased to 70kW by considering ESU may be slowly recharged under hill climbing conditions. Therefore a 70kw fuel cell could be selected for this application.

Beside the 2 second rise time of the output power of the main source, there are two other dynamic factors that generally effect the ESU selection namely cold and hot start characteristics (energy/power requirements, start up time, minimum off time) and operating area. The cold start energy and power requirements determine the minimum amount of energy and power provided by the ESU. In addition, if the cold start-up time is long (several minutes), the ESU must also provide the power of vehicle power train.

The hot-energy start and the power requirement determine the restart fuel penalty that increases fuel consumption and imposes a minimum off time to avoid frequent on and off operations of the main energy source. During the off times, the energy and power required by the vehicle must be provided by the ESU. The system goal is maximum fuel efficiency and minimum ESU weight.

Main energy source accounts for the largest portion of the losses in a vehicle. For example, the fuel cell system in a hybrid electric vehicle accounts for over 60% of the losses. Therefore it is commonly believed that keeping main energy source (fuel cell system) operating at its highest energy point will translate into the vehicle maximum fuel efficiency. However this may not be the case since keeping the main energy source operating at its highest efficiency point implies that the Energy storage unit must provide any extra power required by the vehicle. Consequently, the ESU has to be recharged and this action may produce more losses than allowing the main energy source to operate at a slightly less efficient point than its maximum. Therefore operating area of main energy source is related to the round trip efficiency of the ESU.

Allowing main energy source to operate within a certain range may not only increase system efficiency but also reduce ESU requirements.

3.3.2 Energy Storage Unit

The first step in design of ESU is selection of type of ESU. A battery is a well known energy source used for mass storage of energy. Battery has high energy density but relatively low power density i.e. battery is incapable of supplying a large request of power in short time. Another source available is ultracapacitor. Ultracapacitor has little storage but can supply a large burst of power. Hence an Energy storage unit with combined battery and ultracapacitor can meet both storage and power flow requirement. Battery-ultracapacitor model have advantages such as high peak power capacity, higher efficiency and longer battery runtime when compared to battery alone ESU.

The vehicle power requirement could be ideally expressed as 150kW high 21second long power step [11].After this step the power requirement drops to 54kw when the vehicle reaches 85mph. As mentioned in 4.1 the main energy source has been selected to provide a rated power of 70kW. Assuming that initially the main energy source provides its rated power with no time delay (ideal case) the ESU is required to provide 80kW during 21 seconds yielding a total energy of 467W-h.

In this application a proper combination of batteries and ultracapacitor presents the most light weight solution. Following the iterative sizing procedure in [11] the table V below gives the optimized ESU.

Table V Light Weight Combination of Battery and Ultracapacitor

	BU-ESU	
	Weight(kg)	Volume (l)
Ultracapacitor Pack	56.0	48.0
Battery Pack	144.0	58.0
Total	200.0	106.0

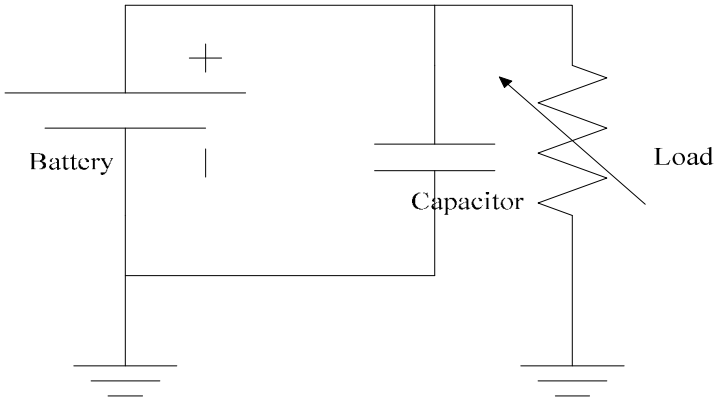

Figure 3.3 Passive Battery/Ultracapacitor Model.

A passive battery/capacitor hybrid, as shown in Figure 3.3 may have several advantages over a battery alone, such as higher peak power capacity, higher efficiency, and longer battery runtime. However, these advantages are limited by the fact that the battery and capacitor are directly connected. Firstly, the battery voltage cannot be different from the capacitor voltage, and so the capacitor array size is determined by the battery voltage since the ultracapacitor has its own upper voltage limit; secondly, the power enhancement of the passive hybrid source is limited by the current distribution between the battery and the capacitor, which is predominantly determined by their respective internal resistances. Under this condition, the battery current may have a large ripple during the pulse period which reaches a maximum value at the end of current pulse. Finally, the terminal voltage of the passive hybrid is not regulated, but instead follows the discharge curve of the battery and can vary considerably between fully charged and fully depleted [12].

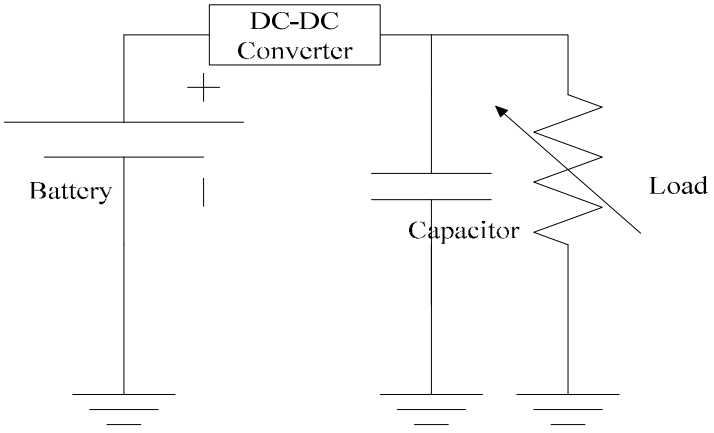

Figure 3.4 An Active Battery/Ultracapacitor/Converter Model.

3.3.3 DC-DC Converter

Adding a bidirectional DC/DC converter between the battery and the ultracapacitor may yield several advantages. The capacitor voltage can be different from the battery voltage, which offers a lot of freedom with respect to design of the battery and capacitor arrays. The power capacity can be much higher than for the passive source because the battery current can be independently limited to a safe value. The power source terminal voltage can be kept relatively constant, with a smaller variation than for the passive source. The efficiency could be improved because the battery operates with lower losses at lower currents, but the tradeoff is against efficiency of the DC/DC converter. With an optimized design, the weight of the power source for a given peak power can be smaller than that of a passive power source for the same load. The DC/DC converter can also serve as the battery charger/controller while the passive hybrid power source requires a separate battery charger.

Ultra capacitor is paralleled with load through another bidirectional DC-DC converter that free wheels the large current and enhances the power.

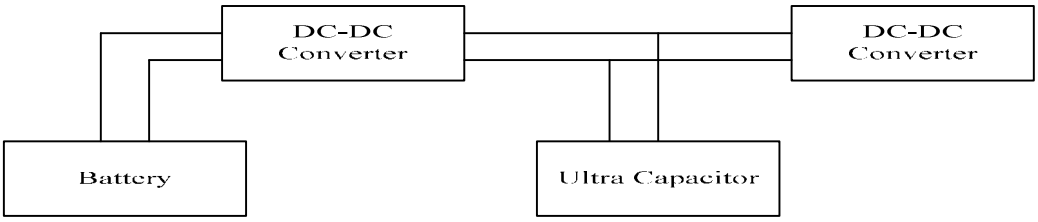

Figure 3.5 Energy Storage Unit Block Diagram.

Table VI DC-DC Converter Design Specifications [13]

Parameter	Value
Maximum Continuous power, P_0	75kW
Rated Output Voltage, V_0	300V
Continuous DC input voltage range, V_i	150-300V
Maximum output voltage ripple, ΔV_0	5%
Maximum input voltage ripple, ΔV_i	5%
Maximum inductor current ripple, r_L	30%
Maximum transfer capacitor voltage ripple ratio , r_C	30%
Switching frequency, f_{SW}	20kHZ

The selected DC-DC converters are half bridge converters. The half bridge converters are capable of determining electric stresses which provide valuable information for component sizing and thermal studies. Also half bridge DC-DC converter presented reduces current stresses on switches, diodes and inductor. It has potential of achieving higher efficiency since it has reduced current levels [13].

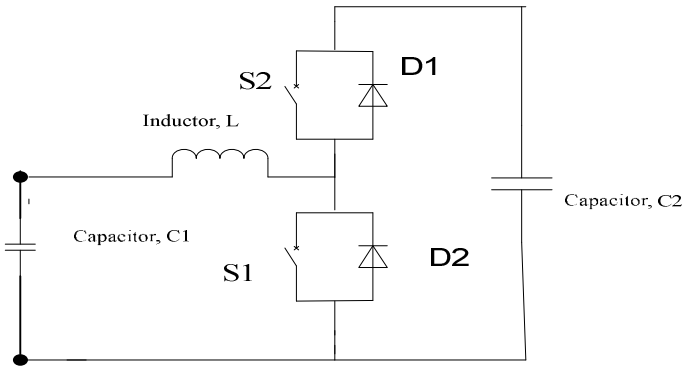

Figure 3.6 Half Bridge DC-DC Converter.

The above Figure 3.6 presents the half bridge DC-DC converter operating as (1) a boost converter when power flows from the ultracapacitor pack to the DC bus (S1 and D1 are active, S2 and D2 are inactive), and (2) a buck converter when power flows from the DC bus to the pack (S2 and D2 are active, S1 and D1 are inactive).

Following the design procedure from [13] the passive component sizes can be determined.

3.3.4 BU-ESU Power Electronics Modeling

The below given table VII is used as base case [14]. The base line system is mid-size SUV whose physical dimensions and performance requirements were already discusses in section 3.3.

Table VII Base table for BU-ESU Power Electronics Modeling

Component	Value
Fuel cell Peak power	70 kW
Fuel cell time response	2s
Battery Weight	144 kg
Ultracapacitor Weight	56kg
BU-converter Power	75kW

3.4 Simulink Model for the Energy Storage Unit

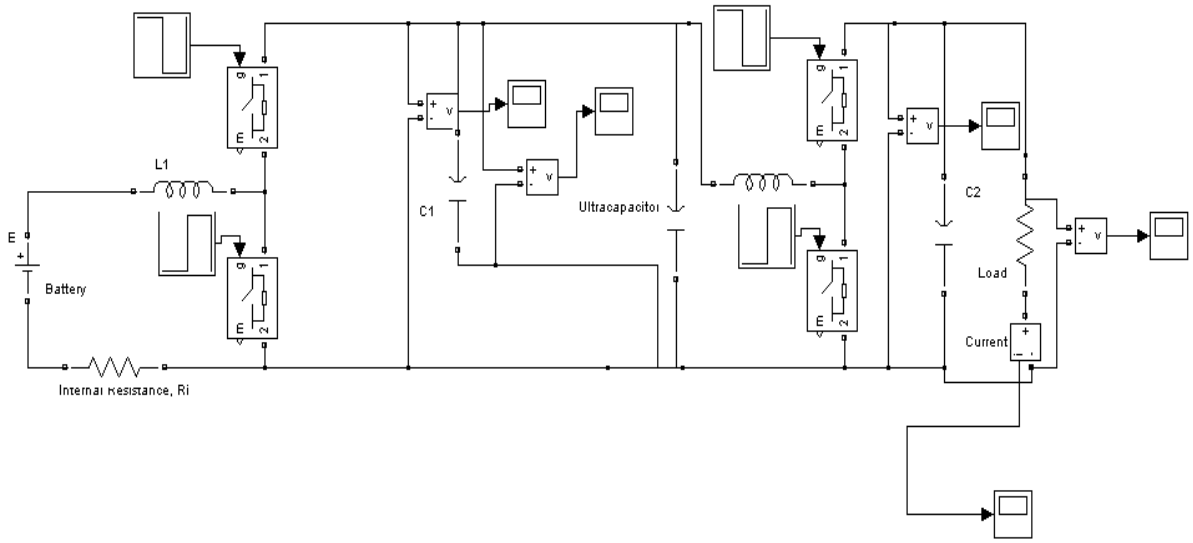

Figure 3.7 Energy Storage Unit with Battery and Ultra capacitor.

The above simulink model (Figure 3.7) is the complete energy storage unit which has a battery, an ultra capacitor and two DC-DC converters as explained in figure 3.5.The components used in the circuit are DC voltage source is 300 volts with and internal resistance of .01 ohms. The inductors (L1=L2) are of 63μH, C1=C2 = 194μF, value of ultracapacitor is 5mF and the load is a constant resistive load of 1ohm. With these values the power of the Energy Storage Unit would be 70kW i.e. the power required by the vehicle under transient conditions as mentioned in section 3.3.2.

3.4.1 Plots for the ESU Model

When the load is of constant resistive type the following graphs for voltage and power (Figure 3.8 and Figure 3.9) are obtained.

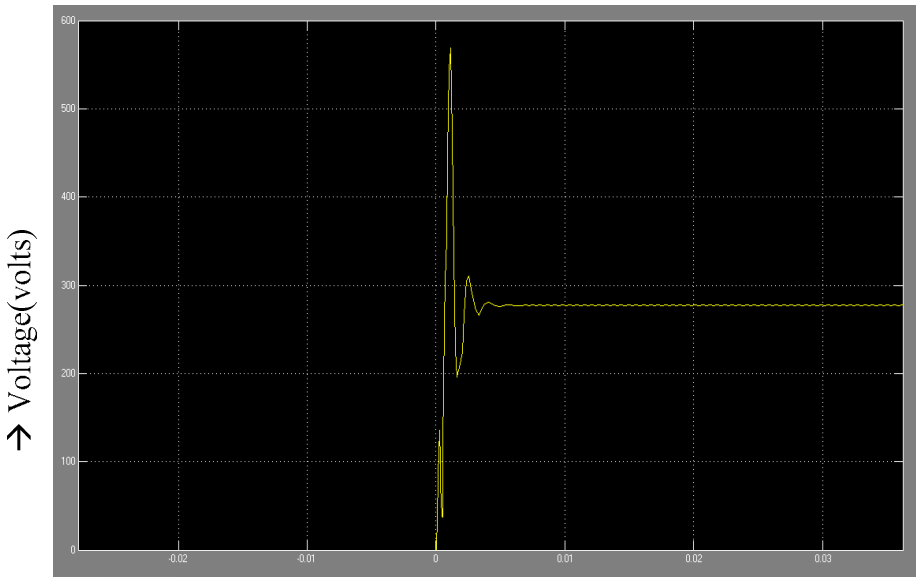

Figure 3.8 Voltage across the Constant Resistive Load.

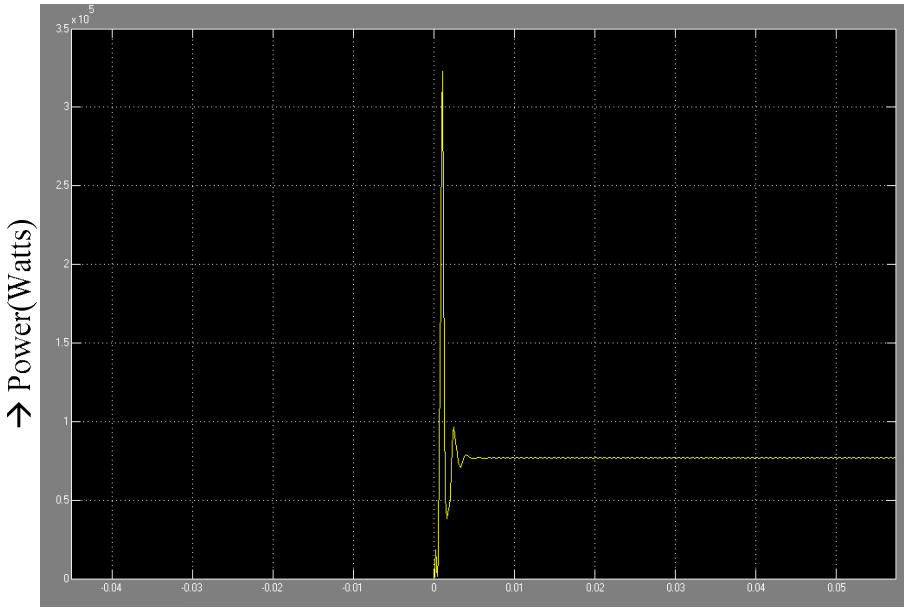

Figure 3.9 Power of the ESU.

When the resistance is varied in steps as shown in the model given below (Figure 3.10) it has been observed that the output voltage and current curves (Figures 3.11 and 3.12 respectively) follow the load (step).

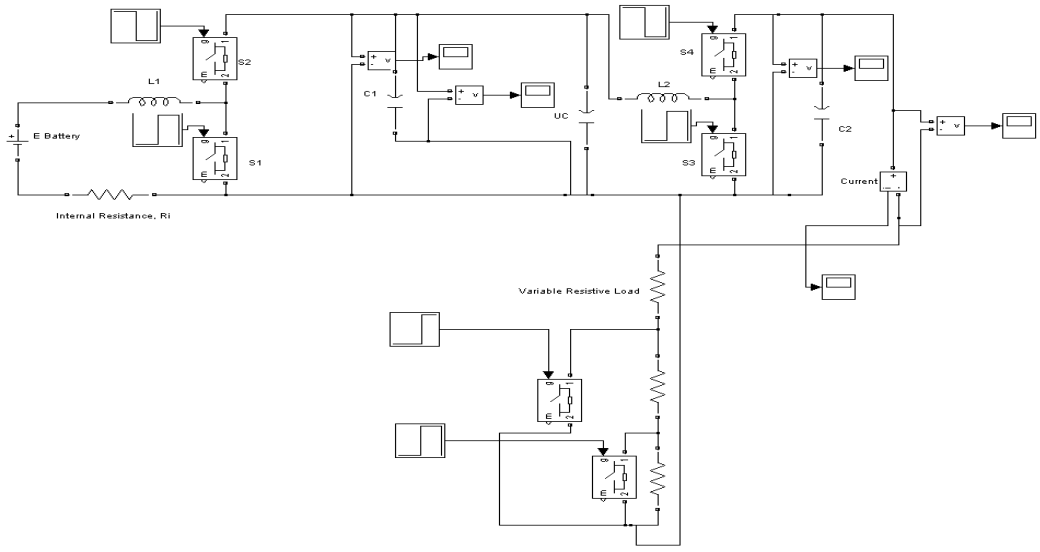

Figure3. 10 Simulink Model for the Energy Storage Unit with Variable Step Load.

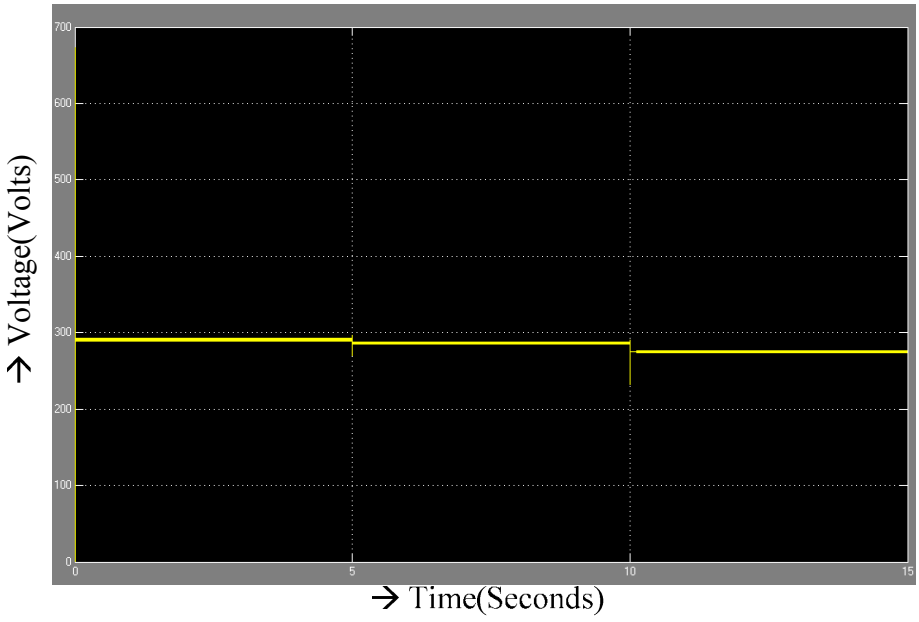

Figure 3.11 Output Voltage of ESU for a Variable Step Load.

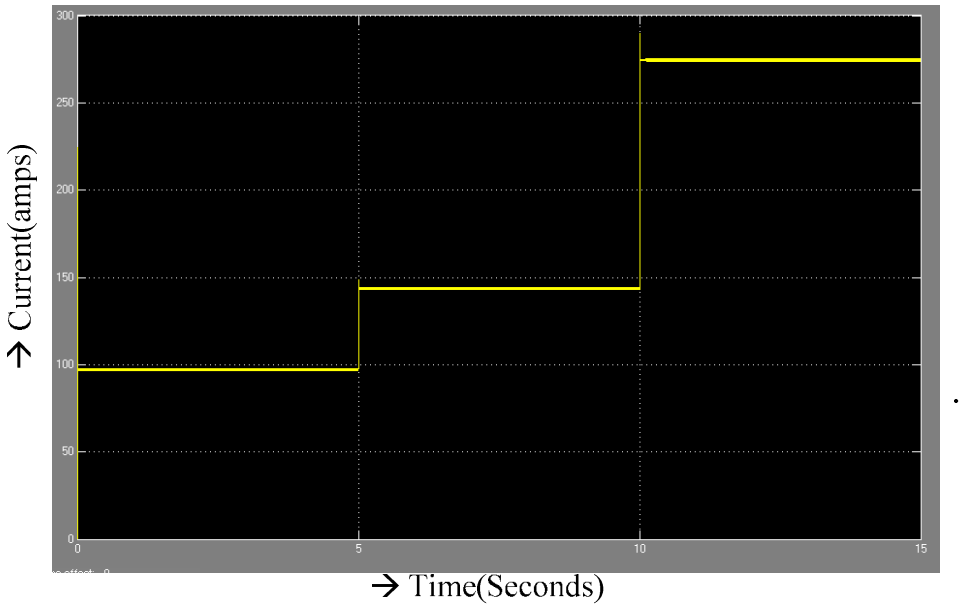

Figure 3.12 Output Current of ESU for a Variable Step Load.

3.5 Parallel Configuration

To observe the load sharing between the PEM and energy storage unit initially the equivalent circuit of PEM has been considered as shown in Figure 3.13 and connected in parallel with a battery. The Figure 3.13 shows the battery in parallel with the equivalent circuit of PEM across the same R-L load.

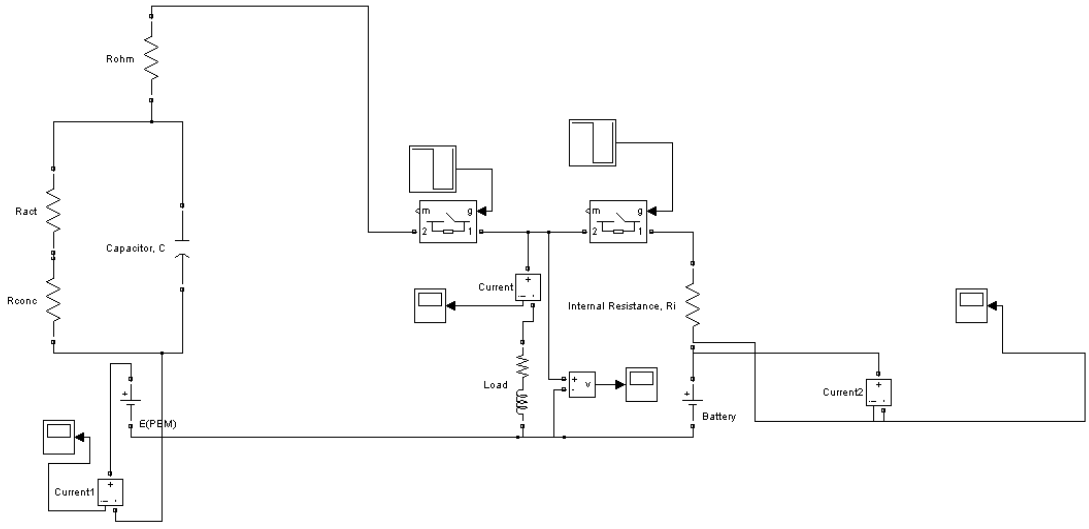

Figure 3.13 Equivalent Circuit of PEM and a Battery sharing the same R-L Load.

Initially the input voltages for both the sources are considered to be equal and the currents at each source (I1 and I2 respectively) are plotted .The current at the load (I3) is also plotted to observe the relation between I1 and I2. The components are V (PEM) = 200V =V Battery, Ri (internal resistance of battery) = .01 ohms, Rconc = .01 ohms, Ract= .2 ohms, Rohmic=.3 ohms, C= 20F, active power at load is .01W and inductive reactive power is 10 vars.

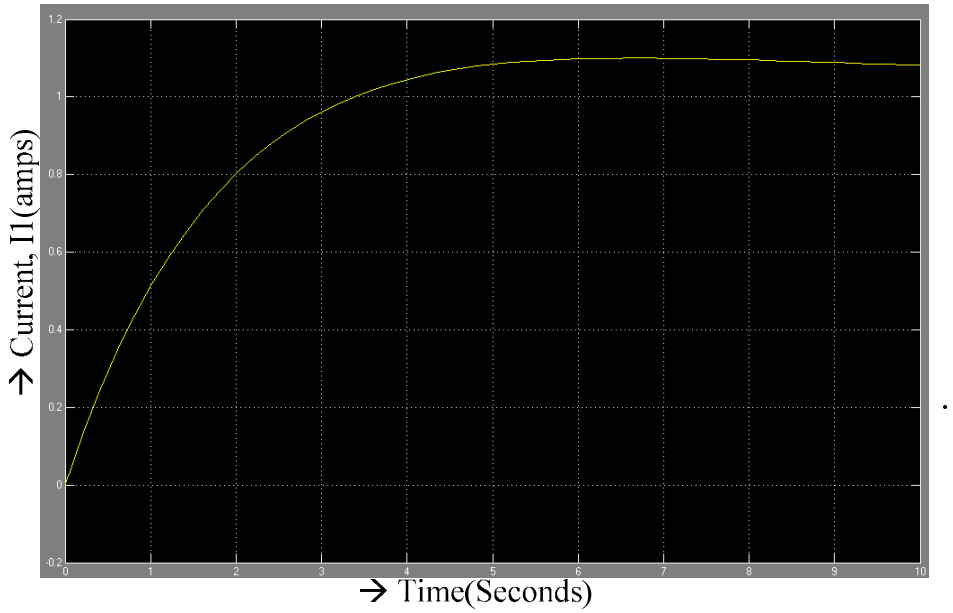

Figure 3.14 Current, I1 at the PEM Fuel Cell.

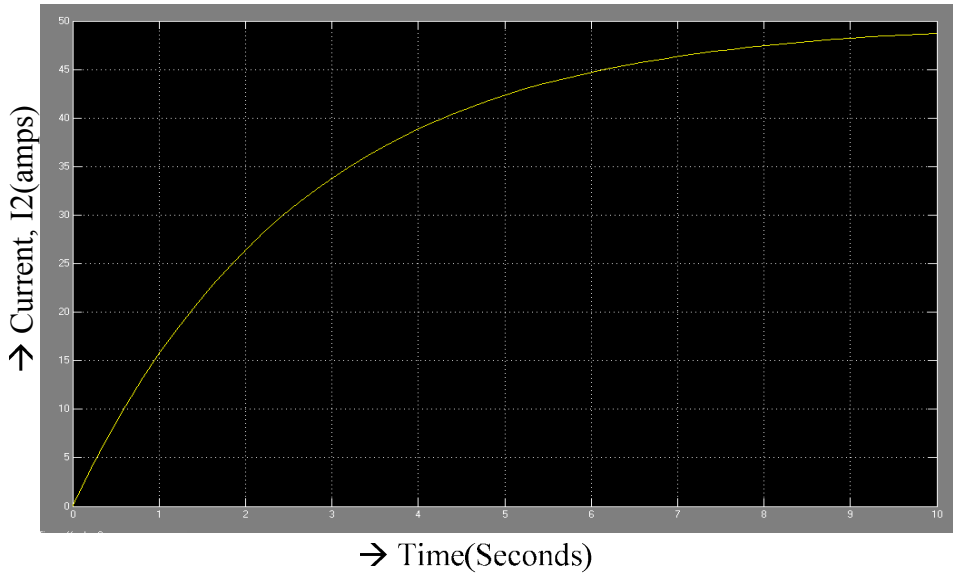

Figure 3.15 Current, I2 at the Battery.

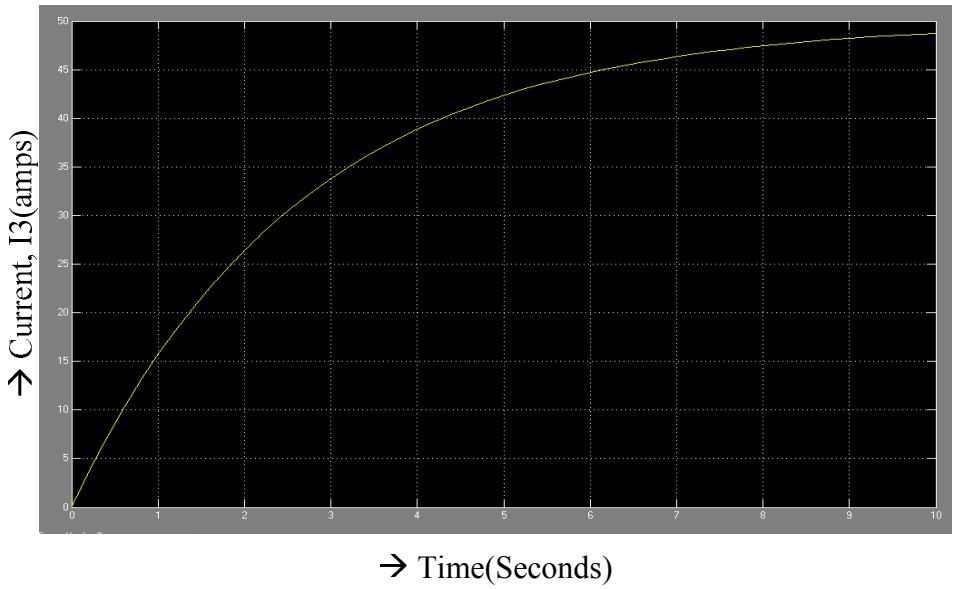

Figure 3.16 Current, I3 at the Load.

From the above graphs (Figures 3.14, 3.15 and 3.16) it can be observed that the load current is sum of the currents at the two sources i.e. I3= I1+I2. Then different voltages are given for both the sources (PEM and Battery) say V (PEM) = 200V and V (battery) = 150V i.e. Voltage given to PEM is higher than the voltage of the battery. All the other components remain the same as mentioned above.

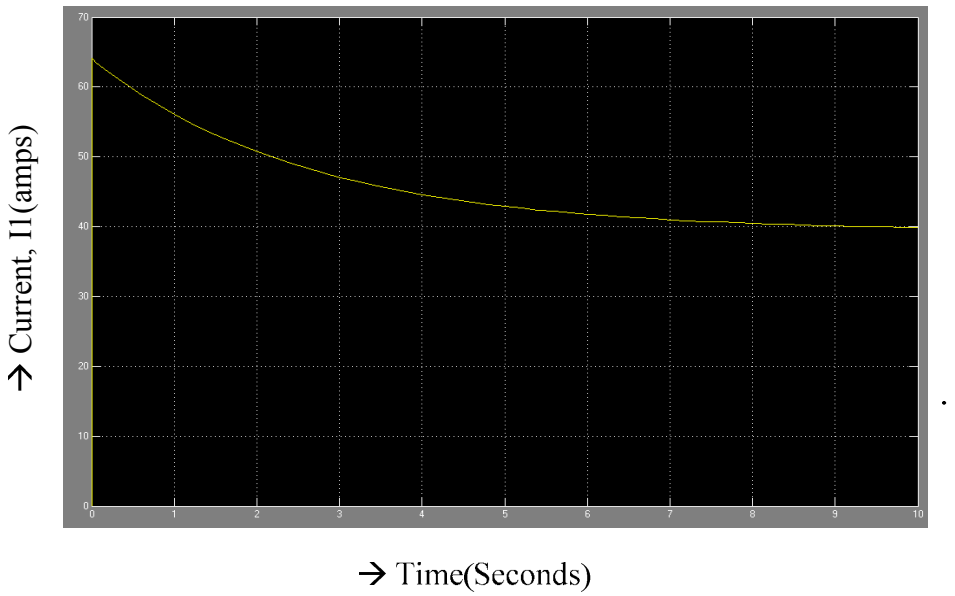

Figure 3.17 Current, I1 at the PEM Fuel Cell (Higher Voltage Source).

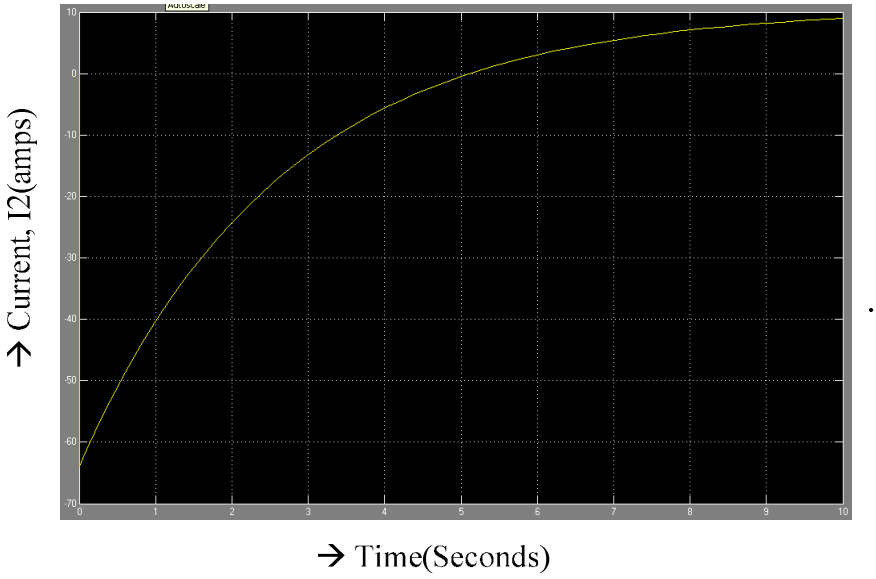

Figure 3.18 Current, I2 at the Battery (Lower Voltage Source).

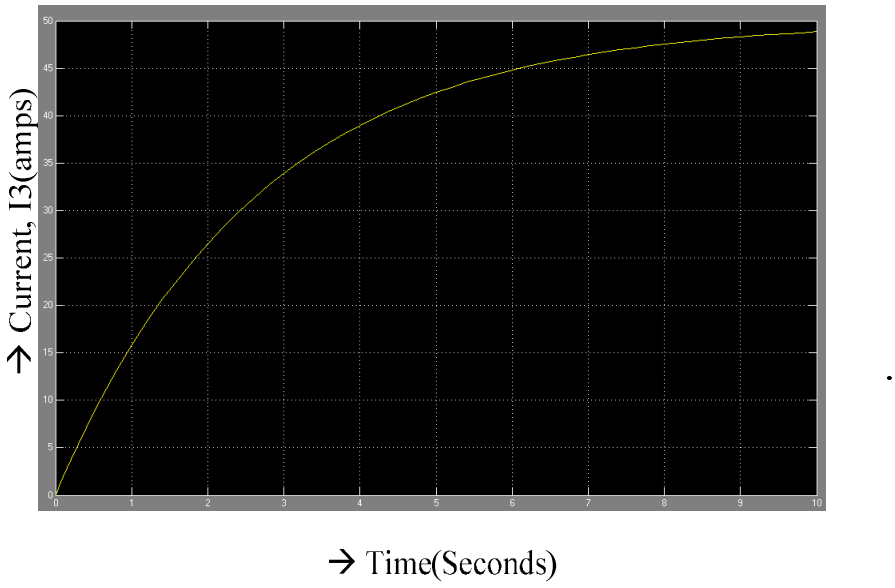

Figure 3.19 Current, I3 at the Load (When PEM and Battery are at different Voltage Levels).

From Figures 3.17, 3.18 and 3.19 it can be observed that when the voltages at the two sources is kept at different levels (PEM is at higher voltage and Battery is at lower voltage when compared to PEM, the current is positive in the PEM and gradually decreases. The current in the

battery is initially negative which indicates that battery gets charged and then it gradually increases. Also the current at the load is observed to be the sum of I1 and I2.

Figures 3.20, 3.21 and 3.22 are the currents I1, I 2 and I3 for a variable step load. It has been observed that I1 is positive and gradually decreasing, I2 indicates the battery is charged initially and the current gradually increases. The current at the load is the sum of I1 and I2.Also all the currents follow the variable step load.

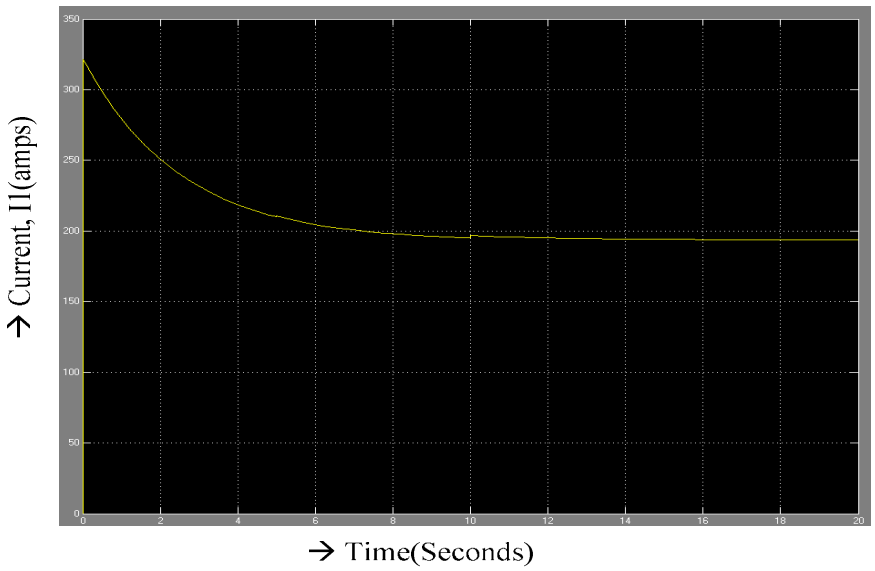

Figure 3.20 Current, I1 at the PEM Fuel Cell for Variable Step Load.

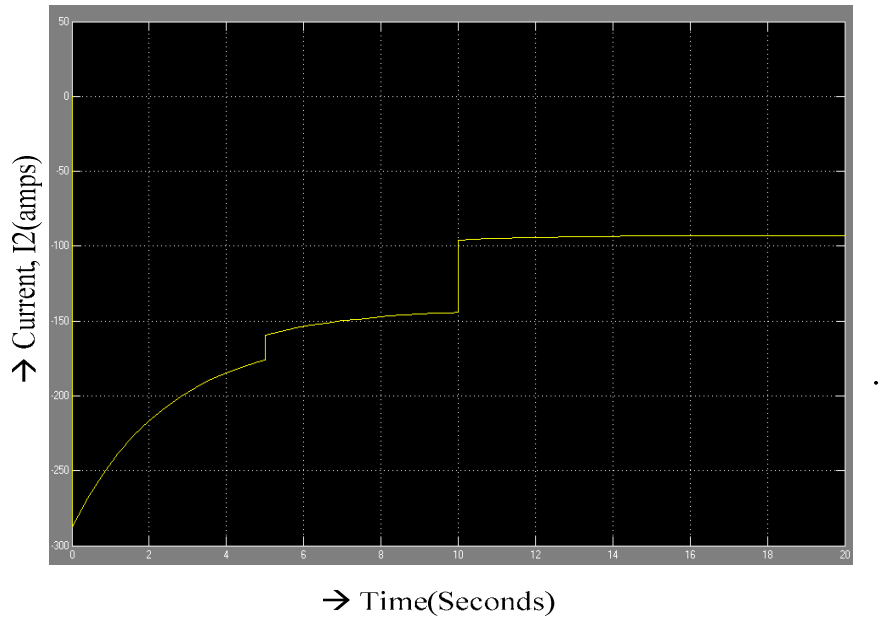

Figure 3.21 Current, I2 at the Battery for Variable Step Load.

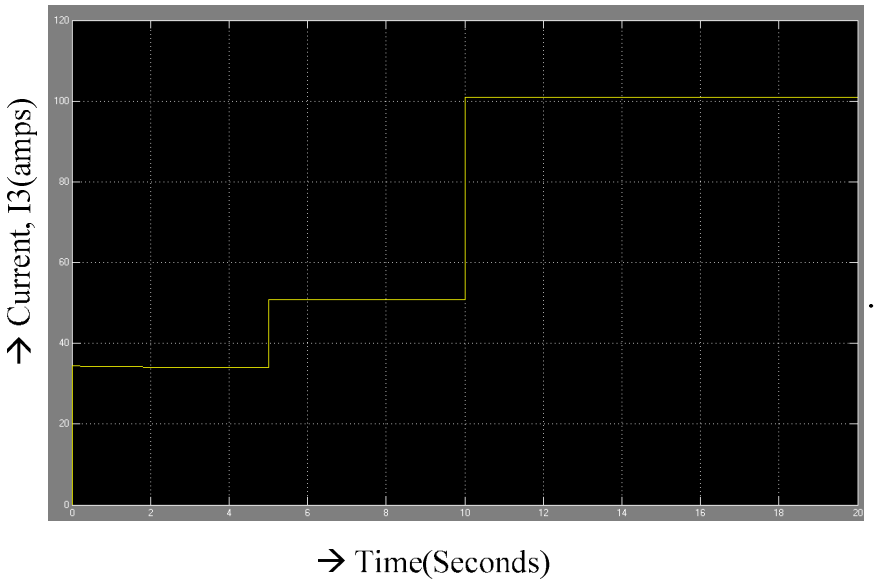

Figure 3.22 Current, I3 at the Step Load.

In all the above simulations (Figure 3.14 to Figure 3.22) the equivalent model of the PEM is considered. Now the actual simulink model of PEM is taken to observe the performance of the parallel model (Figure 3.23).

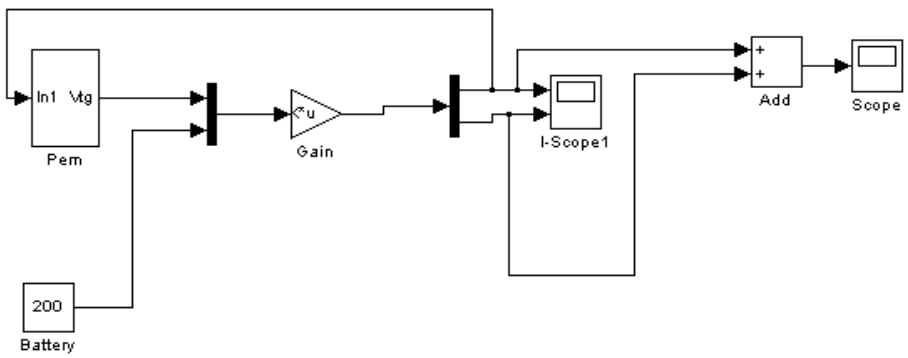

Figure 3.23 Simulink model of the Exact PEM and Battery in parallel across a constant load.

This model is obtained by writing the mathematical equations for the parallel circuit as shown in Figure 3.24.

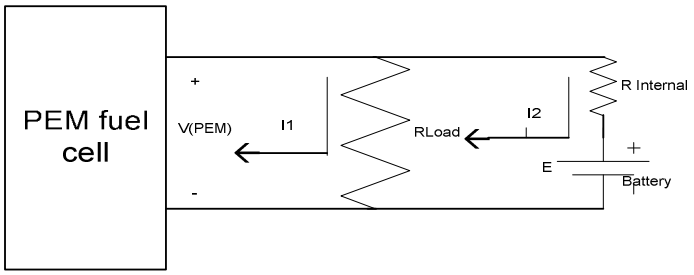

Figure 3.24 Electrical Circuit of a PEM Fuel Cell and Battery in Parallel across a Resistive Load.

V (PEM) = (I1+I2)*Rload

E = I2*Rinternal + (I1+I2)*Rload

Writing above two equations in a matrix form,

$$\begin{bmatrix} V(PEM) \\ \text{E} \end{bmatrix} = \begin{bmatrix} Rload & Rload \\ Rload & Rload + Rinternal \end{bmatrix} \begin{bmatrix} I1 \\ \text{I2} \end{bmatrix}$$

$$\begin{bmatrix} I1 \\ \text{I2} \end{bmatrix} = \begin{bmatrix} Rload & Rload \\ Rload & Rload + Rinternal \end{bmatrix}^{\wedge -1} \begin{bmatrix} V(PEM) \\ \text{E} \end{bmatrix}$$

Hence considering the above two equations a simulink schematic for the parallel circuit using exact PEM model is designed as shown in figure 3.23.The components of the load matrix are Rload = 10ohms, Rinternal = .001.The model is simulated and the currents I1 (Current at PEM fuel cell), I2 (Current at the Battery) and the current at the load (I3) are determined.

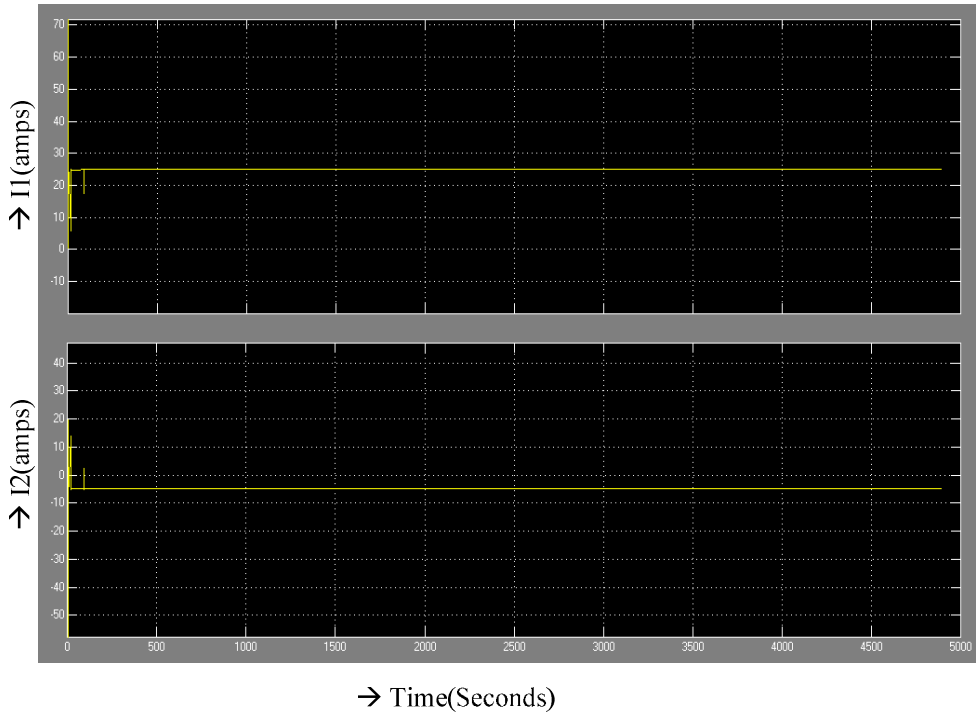

Figure 3.25 Current at PEM Fuel Cell (I1), Battery (I2).

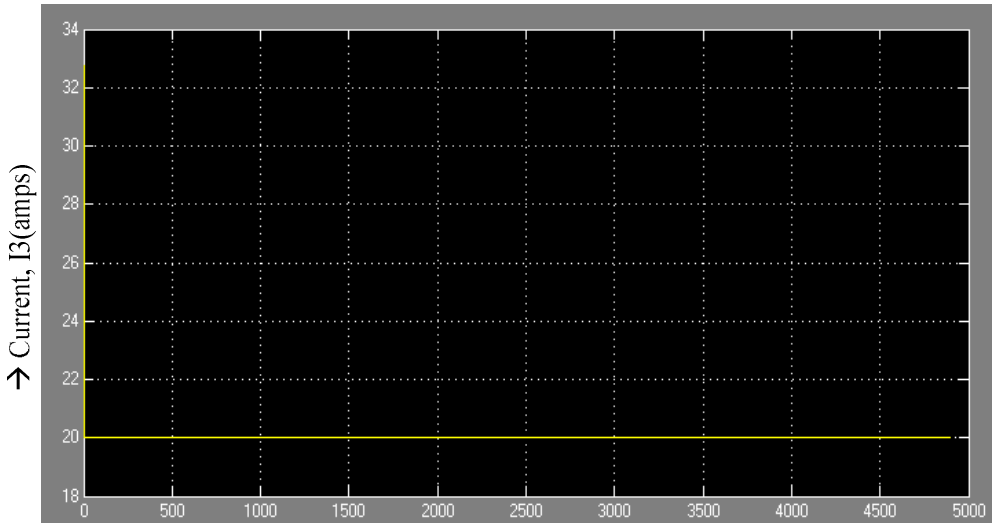

Figure 3.26 Current across the Load, I3.

Chapter 4

CONCLUSION AND FUTURE WORK

4.1 Conclusion

In this report, PEM fuel cell system used for transportation applications is investigated through modeling and simulation. A mathematical model and equivalent model of a PEM fuel cell are studied and the models are validated by comparing the simulations with the experimental results obtained in [6].

Also, the methods of determining energy storage needs and an energy storage unit were investigated. The energy storage unit topology in this report consists of a battery and an ultracapacitor. To determine the size and the most light weight solution for the energy storage unit, the mid size SUV load requirements were studied (The load requirements provided steady state requirement to be met by PEM and the instantaneous requirement to be met by the energy storage unit).

Also two DC-DC converters were modules in simulink and the results of the entire energy storage unit with a battery, an ultracapacitor and two DC-DC converters were observed.

The equivalent model of PEM and battery were connected in parallel across the same load and the load sharing was observed through simulations. Also the exact model of PEM was connected in parallel with a battery and simulated to observe the load sharing.

4.2 Future Work

Based on the results of the study this project leaves a lot of possibilities that can be explored.

1. The project can be extended by considering a dynamic model of the vehicle.
2. The proposed model uses a simple resistive load which can be replaced by an induction motor load.
3. The results obtained are encouraging for further study on parallel configuration of the PEM fuel cell and energy storage unit with suitable control.

References

[1] http://www.esru.strath.ac.uk/EandE/Web_sites/99-00/bio_fuel_cells/groupproject/fuel-cell-Performance/pageframe.htm

[2] http://dodfuelcell.cecer.army.mil/proton.html.

[3] http://americanhistory.si.edu/fuelcells/pem/pemmain.htm.

[4] www1.eere.energy.gov/femp.pdfs/fiemtf-0706.pdf.

[5] Randell S. Gemmen, Parviz famouri, "Electro chemical circuit model of a PEM Fuel Cell", Power engineering society general meeting, 2003, IEEE.

[6] Caisheng Wang; Nehrir, M.H.; Shaw, S.R., "Dynamic models and model validation for PEM fuel cells using electrical circuits" , IEEE transactions on energy conversion, Volume 20, Issue 2, pages 442-451.

[7] Andrew Richard Balkin, "Modelling a 500W Polymer Electrolyte Membrane Fuel Cell", Thesis report submitted to University of Technology, Syden.

[8] www.kettering.edu/~altfuel/fcback.htm.

[9] A. Pesaran, M. Zolot, T. Markel, K. Wipke (NREL), "Fuel Cell/Battery Hybrids: A Review of Energy Storage Hybridization in Fuel Cell Vehicles**"** Presented at 9th Ulm Electrochemical Talks, Ulm, Germany.

[10]Tony Markel, Zolot, Wipke, "Energy storage requirements for hybrid fuel cell vehicles" advanced automotive battery conference June 10-13, 2003.

[11]Schupbach, R.M., Balda, J.C., Zolot, M., Kramer, B., "Design methodology of a combined battery and ultra capacitor energy storage unit for vehicle power management", Power Electronics Specialist Conference,2003, Volume 1, Page(s): 88-93.

[12]Gao, L.; Dougal, R.A.; Liu, S., "Active power sharing in hybrid battery/capacitor power sources", Applied Power Electronics Conference and Exposition, 2003. APEC '03. Eighteenth Annual IEEE Volume 1, 9-13 Feb. 2003 Page(s):497 - 503 vol.1 Digital Object Identifier 10.1109/APEC.2003.1179259.

[13]R M. SCHUPBACHJ., C. BALDA, "Comparing DC-DC Converters for Power Management in Hybrid Electric Vehicles", Electric Machines and Drives Conference, 2003. IEMDC' 03. IEEE International Volume 3, 1-4 June 2003 Page(s):1369 - 1374 vol.3.

[14]Schupbach, R.M. Balda, J.C. “The role of ultracapacitors in an energy storage unit for vehicle power management”, Vehicular Technology Conference, 2003. VTC 2003-Fall. 2003 IEEE 58th Publication Date: 6-9 Oct. 2003 Volume: 5, on page(s): 3236- 3240.